VOLUME 33 | SUPPLEMENT 2 | MARCH 2020

MODERN PATHOLOGY

ABSTRACTS

PEDIATRIC AND PERINATAL PATHOLOGY

(1842-1868)

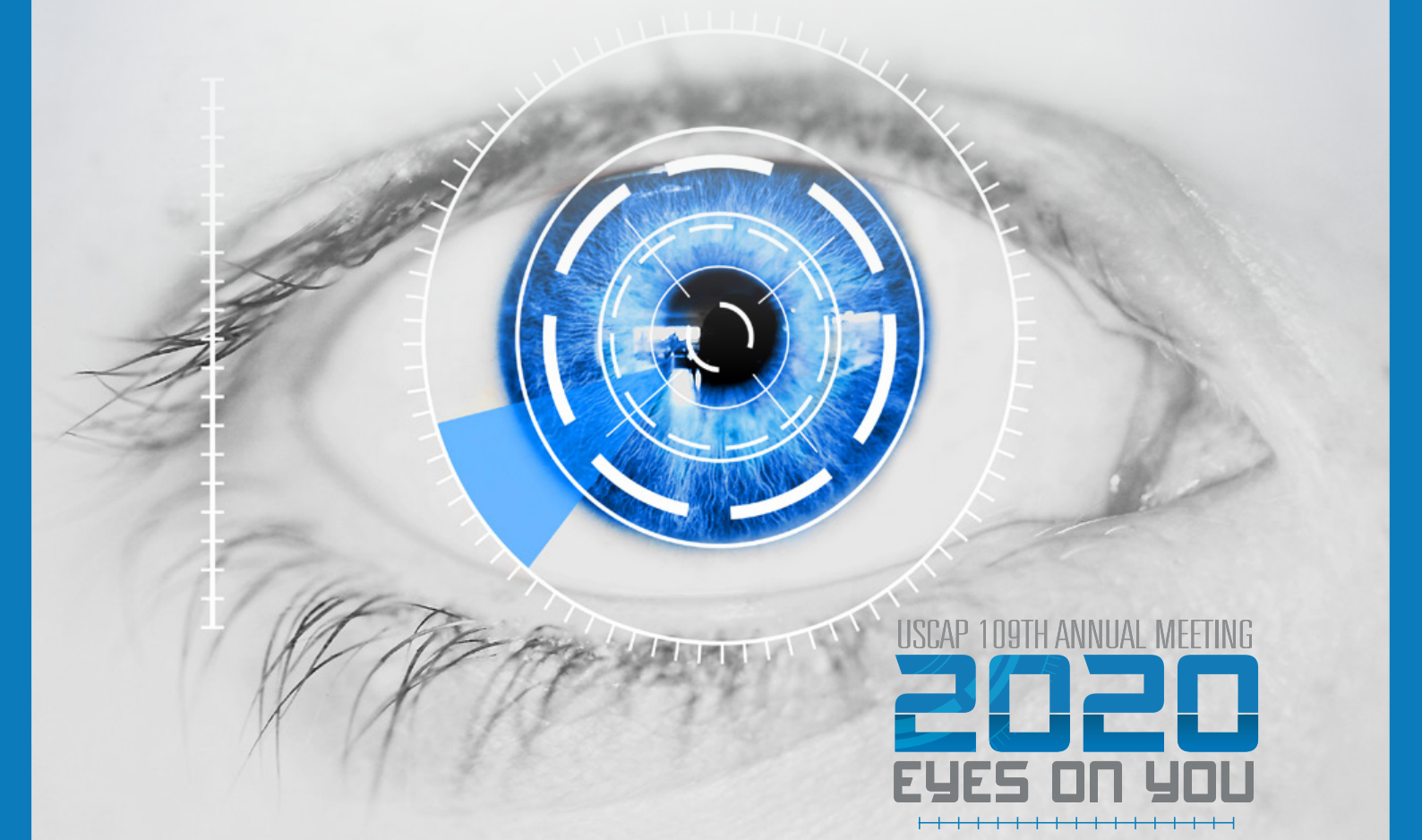

FEBRUARY 29-MARCH 5, 2020

LOS ANGELES CONVENTION CENTER
LOS ANGELES, CALIFORNIA

Published by
SPRINGER NATURE
www.ModernPathology.org

USCAP Creating a Better Pathologist
AN OFFICIAL JOURNAL OF THE UNITED STATES AND CANADIAN ACADEMY OF PATHOLOGY

EDUCATION COMMITTEE

Jason L. Hornick, Chair

Rhonda K. Yantiss, Chair, Abstract Review Board and Assignment Committee

Laura W. Lamps, Chair, CME Subcommittee

Steven D. Billings, Interactive Microscopy Subcommittee

Raja R. Seethala, Short Course Coordinator

Ilan Weinreb, Subcommittee for Unique Live Course Offerings

David B. Kaminsky (Ex-Officio)

Zubair Baloch
Daniel Brat
Ashley M. Cimino-Mathews
James R. Cook
Sarah Dry
William C. Faquin
Yuri Fedoriw
Karen Fritchie
Lakshmi Priya Kunju
Anna Marie Mulligan
Rish K. Pai
David Papke, Pathologist-in-Training
Vinita Parkash
Carlos Parra-Herran
Anil V. Parwani
Rajiv M. Patel
Deepa T. Patil
Lynette M. Sholl
Nicholas A. Zoumberos, Pathologist-in-Training

ABSTRACT REVIEW BOARD

Benjamin Adam
Narasimhan Agaram
Rouba Ali-Fehmi
Ghassan Allo
Isabel Alvarado-Cabrero
Catalina Amador
Roberto Barrios
Rohit Bhargava
Jennifer Boland
Alain Borczuk
Elena Brachtel
Marilyn Bui
Eric Burks
Shelley Caltharp
Barbara Centeno
Joanna Chan
Jennifer Chapman
Hui Chen
Beth Clark
James Conner
Alejandro Contreras
Claudiu Cotta
Jennifer Cotter
Sonika Dahiya
Farbod Darvishian
Jessica Davis
Heather Dawson
Elizabeth Demicco
Katie Dennis
Anand Dighe
Suzanne Dintzis
Michelle Downes
Andrew Evans
Michael Feely
Dennis Firchau
Gregory Fishbein
Andrew Folpe
Larissa Furtado
Billie Fyfe-Kirschner
Giovanna Giannico
Anthony Gill
Paula Ginter
Tamara Giorgadze
Purva Gopal
Anuradha Gopalan
Abha Goyal
Rondell Graham
Alejandro Gru
Nilesh Gupta
Mamta Gupta
Gillian Hale
Suntrea Hammer
Malini Harigopal
Douglas Hartman
John Higgins
Mai Hoang
Mojgan Hosseini
Aaron Huber
Peter Illei
Doina Ivan
Wei Jiang
Vickie Jo
Kirk Jones
Neerja Kambham
Chiah Sui Kao
Dipti Karamchandani
Darcy Kerr
Ashraf Khan
Francesca Khani
Rebecca King
Veronica Klepeis
Gregor Krings
Asangi Kumarapeli
Alvaro Laga
Steven Lagana
Keith Lai
Michael Lee
Cheng-Han Lee
Madelyn Lew
Zaibo Li
Faqian Li
Ying Li
Haiyan Liu
Xiuli Liu
Yen-Chun Liu
Lesley Lomo
Tamara Lotan
Anthony Magliocco
Kruti Maniar
Emily Mason
David McClintock
Bruce McManus
David Meredith
Anne Mills
Neda Moatamed
Sara Monaco
Atis Muehlenbachs
Bita Naini
Dianna Ng
Tony Ng
Michiya Nishino
Scott Owens
Jacqueline Parai
Yan Peng
Manju Prasad
Peter Pytel
Stephen Raab
Joseph Rabban
Stanley Radio
Emad Rakha
Preetha Ramalingam
Priya Rao
Robyn Reed
Michelle Reid
Natasha Rekhtman
Jordan Reynolds
Michael Rivera
Andres Roma
Avi Rosenberg
Esther Rossi
Peter Sadow
Steven Salvatore
Souzan Sanati
Anjali Saqi
Jeanne Shen
Jiaqi Shi
Gabriel Sica
Alexa Siddon
Deepika Sirohi
Kalliopi Siziopikou
Sara Szabo
Julie Teruya-Feldstein
Khin Thway
Rashmi Tondon
Jose Torrealba
Andrew Turk
Evi Vakiani
Christopher VandenBussche
Paul VanderLaan
Olga Weinberg
Sara Wobker
Shaofeng Yan
Anjana Yeldandi
Akihiko Yoshida
Gloria Young
Minghao Zhong
Yaolin Zhou
Hongfa Zhu
Debra Zynger

To cite abstracts in this publication, please use the following format: **Author A, Author B, Author C, et al. Abstract title (abs#). In "File Title."** ***Modern Pathology*** **2020; 33 (suppl 2): page#**

1842 Mutation Landscape of Primary and Recurrent Malignant Rhabdoid Tumors

Brooj Abro[1], Madhurima Kaushal[2], Louis Dehner[2], John Pfeifer[3], Mai He[2]
[1]Washington University in St. Louis, St. Louis, MO, [2]Washington University School of Medicine, St. Louis, MO, [3]Washington University, St. Louis, MO

Disclosures: Brooj Abro: None; Madhurima Kaushal: None; Louis Dehner: None; John Pfeifer: *Stock Ownership*, PierianDX; Mai He: None

Background: Malignant rhabdoid tumors (MRT) are rare and aggressive solid tumors affecting mainly the pediatric population with dismal clinical outcomes. Although most commonly described in the central nervous system (atypical teratoid rhabdoid tumors, AT/RT) and kidney, these tumors occur throughout the body. Regardless of the sight of origin, mutations involving *SMARCB1 (INI1)* are characteristic of this malignancy, which is considered the driver mutation. In our previous study, we investigated immune-checkpoint markers in MRT and also studied the tumor mutation burden which was found to be low, except in one case. In this study we investigated the mutation landscape of these tumors.

Design: Genomic DNA was extracted from FFPE tissue. Whole-exome sequencing was performed on the initial tumor and metastatic samples. Total 8 cases were sequenced (3 pairs with both primary and recurrent/metastatic tumor and 2 cases with only primary tumor). Sequencing targeted 25-30M reads for normal tissue and 45-50M reads for neoplastic tissue. Raw sequencing data was processed and variant score recalibration was done according to the GATK1 v 3.3.0 best practices recommendations. Mutation analysis and somatic mutation discovery for single nucleotide variants (SNVs) was performed using MuTect v1.1.42; Indel calling and somatic indel identification was performed using the GATK IndelGenotyper tool v2. SNVs and Indels were then annotated using Annovar3.

Results: All cases had germline *SMARCB1* mutations. Multiple somatic mutations were identified involving a total of 60 genes (Figure 1). The number of genes involved ranged from 5 to 16 in primary tumors and 16 to 29 in recurrent/metastatic tumors. Majority of the genetic alterations were missense mutations. Nonsense, frameshift, splice site, insertions and deletions were among the less frequently observed mutations. Significant variation was seen in the mutation landscape among different MRT cases with a few recurrent mutations identified involving *MUC4, MUC12, CLCNKA, DDX11, FCGBP and BCLAF1*. Recurrent/metastatic tumors also showed variations in mutation landscape when compared to their primary counterparts, showing both lack of some variants and acquisition of new mutations.

Figure 1 - 1842

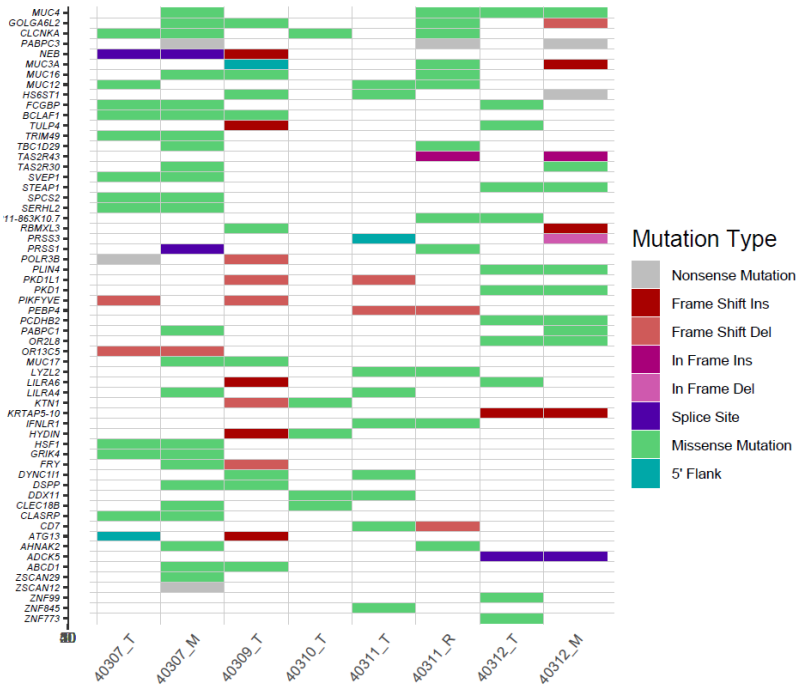

Figure 1: Mutations identified in MRT cases (n=8). Each case is represented by the sequencing number. T= primary tumor, M= metastatic, R= recurrent.

Conclusions: Even though MRTs are characterized by strong driver mutations, there is significant variation in the spectrum of mutations among various cases. Exploring the genetic landscape of these tumors can help identify new targets for therapy.

1843 The Role of Hypoxia-Inducible of Y5 Receptor in Bone Dissemination of Ewing Sarcoma – A Mouse Xenograft Model

Mina Adnani[1], Susana Galli[2], Sung-Hyeok Hong[3], Joanna Kitlinska[3]
[1]Georgetown University Medical Center, [2]Georgetown University Medical Center, Rockville, MD, [3]Georgetown University Medical Center, Washington, DC

Disclosures: Susana Galli: None; Sung-Hyeok Hong: None

Background: Ewing Sarcoma (ES) is known as the second prevalent malignant bone tumor after osteosarcoma in children and adolescents. The main strategy for treatment in patients with metastatic ES is surgery, radiotherapy and chemotherapy. Unfortunately, the survival rate of ES patients with metastases, particularly to bone, is still very poor after these treatments. Thus, there is a need for new therapeutic solutions for patients with ES bone metastatic disease. Our previous research has shown that ES cells constitutively express high levels of NPY and its receptors Y1R and Y5R. Hypoxia is a characteristic feature of growing solid tumors and we have shown previously that NPY increases tumor cell motility and invasiveness via activation of the Y2R/Y5R axis under these conditions.

Design: We investigated the role of Y5R in ES bone metastases by using ES cell line (SK-ES-1) that disseminates to bone. To this end, we used inducible CRIPSR/Cas9 system to create an SK-ES-1/Y5R knockout cell line to be used as a xenograft in *in vivo* experiments. Since the system we used was doxycycline (Dox)-inducible, thus the group of mice that did not receive Dox in their diet served as our control group. Moreover, to create hypoxic conditions, we performed Femoral Artery Ligation surgery (FAL). In our previous experiments, FAL exacerbated SK-ES1 bone metastasis. In these *in vivo* experiments, three main experimental groups were compared: Wild Type SK-ES1, SKES-1 /sgY5R-DOX and SKES-1/sgY5R+DOX. Each group receiving the genetically engineered cell line was divided into two subgroups: with and without FAL surgery.

Results: As expected, FAL increased frequency of bone metastases in control mice and SKES-1 /sgY5R-DOX groups, while in the group with SKES-1/sgY5R+DOX, the Y5R knockout prevented this effect. Moreover, majority of metastases arising in SKES-1/sgY5R+DOX mice were initiated by the clones of ES cells without Y5R gene modification, as indicated by DNA sequencing, further confirming the role of Y5R in ES dissemination. To confirm these results, we performed immunohistochemistry and Western blot with Y5R antibody in primary tumor and all metastatic tissues.

Conclusions: This data suggests that Y5R receptor plays an important role in Ewing Sarcoma metastasis, especially in hypoxia-induced bone dissemination. Therefore, targeting Y5R receptor may be a new therapeutic path for patients with ES bone metastases.

1844 Morphologic and Flow Cytometric Discordances in Bilateral Pediatric Bone Marrow Biopsies

Aadil Ahmed[1], Christopher Tormey[1], Alexa Siddon[2]
[1]Yale University School of Medicine, New Haven, CT, [2]Yale University School of Medicine, Westbrook, CT

Disclosures: Aadil Ahmed: None; Christopher Tormey: None; Alexa Siddon: None

Background: Bilateral bone marrow sampling is recommended for staging of lymphoma and solid organ malignancies, however, only few studies have evaluated the actual morphologic and/or flow cytometric differences. The study aims to review the utility of bilateral sampling of bone marrow in pediatric population by evaluating disagreements between contralateral biopsies.

Design: We performed a retrospective review of the institutional pathology database for bilateral bone marrow sampling performed on pediatric patients (0-19 years) between 1/2000-7/2019.

Results: A total of 1669 pediatric bone marrow biopsies were performed during the study period out of which 376 biopsies were performed bilaterally on 269 patients for various hematologic and non-hematologic disorders (Figure 1). Only 2 samples were considered suboptimal for diagnosis while unilateral inadequacy was seen in 16 samples (4%). 80% (n=303) of the biopsies revealed negative findings whereas overall positivity for bilateral disease was 12% (n=47). Among samples with bilateral disease, 7 cases showed more than 10% difference in involvement of contralateral biopsies. Twenty-six (7%) samples showed unilateral disease and 4/26 contralateral biopsies in this group were inadequate. The cases with unilateral disease included neuroblastoma (13), rhabdomyosarcoma (7), Ewing sarcoma (3), Hodgkin (2) and Burkitt lymphoma (1). More than half 14/26 of these biopsies were performed for follow-up of residual or recurrent disease. While flow cytometry findings were largely concordant, 2 cases with negative morphologic findings showed 1% residual lymphoblastic leukemia in one case and incidental 1% monoclonal B-cells in another staging marrow for rhabdomyosarcoma.

Figure 1 - 1844

Characteristics and Indications of Pediatric Bilateral Bone Marrow Samples

N (samples): 376 n (patients): 269 Mean age: 9 years Male: 137, Female: 132

Primary Diagnostic: 36, Follow-up for residual/recurrence: 105, Staging: 235

Aspirate: 4, Core: 149, Both: 223

Clinical Indications

Hematologic:

Hodgkin Lymphoma 70
B-cell Lymphoma (DLBCL, Marginal, Primary Mediastinal/CNS) 21
T/B Acute Lymphoblastic Leukemia 18
Burkitt 17
Cytopenia 17
T-cell Lymphoma 5
Acute Myeloid Leukemia 5
Mastocytosis 1

Non-Hematologic:

Neuroblastoma 114
Rhabdomyosarcoma 61
Ewing Sarcoma 34
Unknown malignancy with metastasis 3
Osteosarcoma 2
Fibrosarcoma 1
Desmoplastic small round cell tumor 1
MPNST 1
LCH 1
Xanthogranuloma 1
Gaucher 1
Sarcoidosis 1
Ectomesenchymoma 1

Conclusions: Based on our data, the probability of difference in results between contralateral bone marrow biopsies is approximately 6%. While ancillary studies should reduce the need for bilateral sampling in hematologic disorders, a risk-stratified approach based on clinical and radiologic correlation and use of molecular studies should be used in solid organ tumors that can help reduce the cost and time associated with bilateral biopsies.

1845 Should all EWSR1-Rearranged Neoplasms be Classified and Treated as Ewing Sarcoma?

Monica Aldulescu[1], Pauline Chou[2], Nitin Wadhwani[3]
[1]Chicago, IL, [2]Lurie Children's Hospital of Chicago, Chicago, IL, [3]Lurie Children's Hospital, Chicago, IL

Disclosures: Monica Aldulescu: None; Pauline Chou: None; Nitin Wadhwani: None

Background: EWSR1 gene is known to be rearranged in a diverse set of tumours. While the development of molecular testing techniques has allowed better categorization malignant neoplasms, the caveat that comes with this, is occasional discrepant results between how a tumour appears morphologically and the resultant molecular rearrangement. Herein, we would like to describe three unique cases with an atypical clinical and histological presentation, which displayed rearrangement of the EWSR1 gene.

Design: Case 1 is from a 13 year-old female who presented with headaches and proptosis of her left eye, with imaging studies showing a soft tissue mass involving the superior nasal cavity. Histologic sections showed an infiltrative tumor with lobular architecture containing foci of necrosis, increased cellularity, and a background of lace-like osteoid.

Case 2 is from a 13 year-old male presenting with a large extra-axial lesion with calvarial involvement. Histologic sections from the tumor showed bland appearing round cells and intersecting fascicles of spindled cells with scant eosinophilic cytoplasm.

Case 3 is that from a 14 year-old female presenting with a chest wall mass, in which histologic sections demonstrated a primitive tumor with neural differentiation, that was difficult to classify as the tumor was negative for CD99 and positive for SOX-10.

Results: Case 1 showed that the tumor cells showed non-specific CD99 staining and in-house fusion detection panel showed a EWSR1-CREB3L1 fusion transcript with high read counts (>40,000). The presence of this fusion transcript was also confirmed in a separate PCR amplification reaction.

Case 2 showed that the tumor cells were positive for CD99, and tumor-only sequencing demonstrated a fusion between the EWSR1 gene on chromosome 22q12 and the BEND2 gene on chromosome Xp22. Given this, the categorization of this tumor was questionable, as it can

either be classified as a Ewing Sarcoma with a novel mutation, or a mesenchymal, non-meningothelial tumor (dural-based sarcoma) with EWSR1-BEND2 fusion.

Case 3 was also difficult to classify as the tumor was negative for CD99 and positive for SOX-10. NGS testing and subsequent RT-PCR showed EWSR1-FLI1.

Conclusions: These cases are unique, in that they do not fit the usual morphologic and immunohistochemical features of either Ewing or Ewing-like sarcoma, and therefore begs the question: Given the presence of these molecular rearrangements, should these tumors still be classified and treated as Ewing Sarcoma?

1846 Congenital Letterer-Siwe disease (Langerhans Cell Histiocytosis): Unique Case Presenting as Intrauterine Fetal Demise

Ayesha Baig[1], Steffen Albrecht[2], Moy-Fong Chen[3]
[1]McGill University, Montréal, QC, [2]Montreal Neurological Hospital, Montreal, QC, [3]McGill University Health Center, Montréal, QC

Disclosures: Ayesha Baig: None; Steffen Albrecht: None; Moy-Fong Chen: None

Background: Langerhans cell histiocytosis (LCH) is a spectrum of disorders resulting from clonal proliferation of Langerhans cells. Letterer-Siwe disease is a multi-systemic type of LCH occurring in children younger than 2 years of age. It typically manifests with multifocal cutaneous lesions, hepatosplenomegaly, lymphadenopathy, pulmonary lesions and destructive osteolytic bone lesions. We present a case of Letterer-Siwe disease in a stillborn.

Design: A 32-week stillborn female was born to a 21-year-old G2A1. The fetus was well developed and appropriate for gestational age but mildly hydropic and pale. The skin showed severe maceration with multiple targetoid lesions over the face, trunk, and limbs. On autopsy, hepatosplenomegaly was identified. The brain was very pale and the placenta was large and bulky.

Results: Despite severe autolysis, histological examination showed disseminated histiocytes with multinucleated giant cells in the skin, lungs, thymus, mesenteric lymph nodes, spleen, and brain. By immunohistochemistry, the histiocytes were positive for CD1a, S100, and Langerin (CD207), confirming the diagnosis of LCH. There was also splenic and cerebral extra-medullary hematopoiesis and marked erythropoiesis in the placenta. The BRAFV600E variant assay performed on DNA extracted from thymus was negative.

Conclusions: This case is very rare. Only one other case was reported in the English language to our knowledge with the presentation at term; in that case, the brain was apparently not involved and the placenta showed no significant change. Unfortunately, the family and obstetric histories are lacking in our case. Letterer-Siwe disease is poorly understood, further studies, especially molecular and genetic studies are necessary.

1847 Impact of Age on Submucosal Nerve Diameter in Rectal Biopsies from Patients with Hirschsprung Disease

Sarah Beach[1], Fang Bu[2], Selene Koo[2], Michael Arnold[3], Miriam Conces[2]
[1]The Ohio State University, Columbus, OH, [2]Nationwide Children's Hospital, Columbus, OH, [3]Children's Hospital Colorado, Denver, CO

Disclosures: Sarah Beach: None; Fang Bu: None; Selene Koo: None; Michael Arnold: None; Miriam Conces: None

Background: Hypertrophic submucosal nerves, defined as ≥40 microns in diameter, are considered supportive of a diagnosis of Hirschsprung disease (HSCR), but the effect of age on nerve diameter has not been well-studied. We sought to determine the distribution of nerve diameter in ganglionated rectal biopsies and the significance of hypertrophic submucosal nerves in the diagnosis of Hirschsprung disease based on age.

Design: Rectal biopsies performed at our institution in the evaluation of Hirschsprung disease from 2017-2018 were retrospectively collected and reviewed. Hirschsprung disease status was determined by the presence or absence of ganglion cells. The diameter of the largest submucosal nerve was measured and compared between age groups.

Results: Within the 2 year period, 179 rectal biopsies with adequate submucosa were identified. Ganglion cells were present in 151 biopsies, and 28 aganglionic biopsies were diagnosed as Hirschsprung disease. Submucosal nerve diameter range was 17.5 - 101.5 microns in non-Hirschsprung disease biopsies (non-HSCR) and 35 - 98 microns in HSCR biopsies (Figure). Across all ages, hypertrophic submucosal nerves were significantly associated with Hirschsprung disease [HSCR = 25/28 (89.3%) vs non-HSCR = 59/151 (39.1%), p=<0.0001] and showed a sensitivity of 89.29% and specificity of 60.93%. Stratified by age, the submucosal nerve diameter remained statistically significant for HSCR in patients <1 year of age [HSCR = 22/24 (91.7%) vs non-HSCR = 19/91 (20.9%), p=<0.0001] with

sensitivity of 91.67% and specificity of 79.12%. Hypertrophic submucosal nerves were not statistically significant in patients ≥1 year of age [HSCR = 3/4 (75%) vs non-HSCR = 40/60 (66.7%), p=1] and showed reduced sensitivity (75%) and specificity (33.33%) for the diagnosis of HSCR. Based on a receiver operating characteristic curve, a nerve diameter of 45 microns demonstrates the greatest sensitivity (88%) and specificity (83%) for HSCR.

Figure 1 - 1847

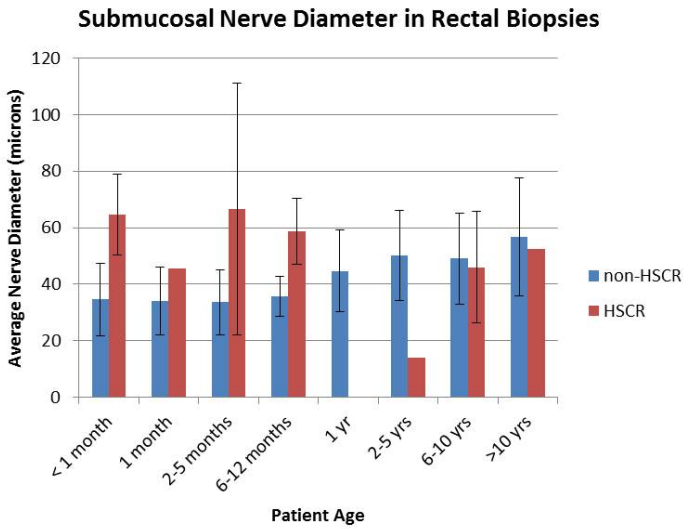

Conclusions: The average submucosal nerve diameter in non-HSCR rectal biopsies increases with age. Hypertrophic submucosal nerves are significantly associated with HSCR in patients <1 year of age but may have limited utility for the diagnosis of HSCR in patients >1 year of age. However, our data includes very few patients >1 yr, and additional studies are needed to evaluate biopsies from older children.

1848 Genetic Variants in Hirschsprung's Disease Patients of the Indian Cohort

Maria Bukelo[1], Usha Kini[2]
[1]St. John's Medical College, Bangalore, Karnataka, India, [2]Bangalore, India

Disclosures: Maria Bukelo: None; Usha Kini: None

Background: Hirschsprung disease(HD) is a congenital disorder characterized by varying degrees of intestinal aganglionosis. Its incidence varies from 1/10,000 live-births in Hispanics to 2.8/10,000 live-births in Asians. Of all the 15 genes implicated in HD, defects in the RET gene play a major role with 50% being familial and 7%-35% sporadic. However, there is no such data in the Indian population. Studying the association of the RET gene in the Indian population is essential for understanding the pathogenesis of the disease and to estimate recurrence risk rates in our population. Hence we decided to study the association of the RET gene, it's ligand GDNF and associated signaling pathway EDNRB and EDN3 with HD in our cohort.

Design: Exome sequencing of RET, EDNRB, GDNF and EDN3 on an NGS platform (Ion PGM) had been performed on genomic DNA from 91 patients and 7 trios (proband+parents). The primer panel had been designed with reference to the human genome (hg38) with a target size of 27.2kb made up of 102 amplicon (in 2 pools) ranging in size of 125-375bp with a coverage of 98.5%. All genes were sequenced for an average of 500x coverage. The data from seven sequencing runs were analyzed using the Torrent Suite V5 analysis pipeline and annotated using Ion Reporter Software v5.12 (Life Technologies, CA, USA) as shown in Figure 1.

Results: Of the 98 cases (55 short segment, 27 long segment and 16 TCA) sequenced in 75 males and 23 females, there were 8 missense mutations on RET, 5 missense mutations on EDN3, 3 mutations on EDNRB and one missense mutation on GDNF. Of the 8 missense mutations on RET, 4 are known and 4 are novel. Of the 4 novel variants, 2 are located on the Ca2+ binding motif and are likely pathogenic. Sequence alignment studies for the rest of the 2 novel variants suggested that one was an un-conserved residue and the other was a conserved residue. The variant on GDNF is likely pathogenic. The variants on EDNRB and EDN3 were of uncertain significance. There was no significant correlation between the variants noted and HD phenotype.

Figure 1 - 1848

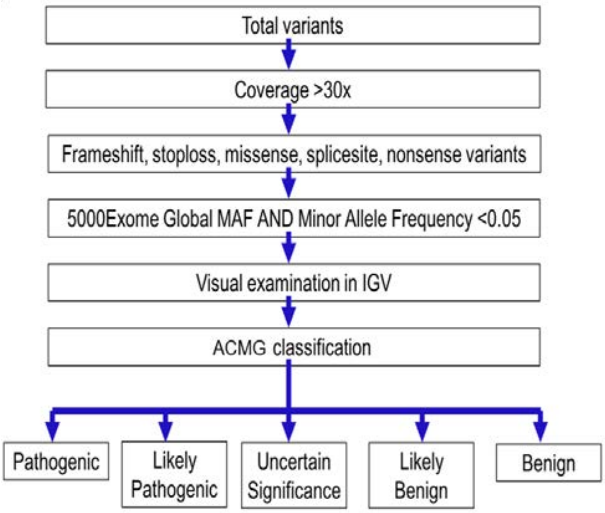

Conclusions: RET is the most commonly involved gene in the HD patients of the Indian cohort with no clinical correlation to the disease phenotype.

1849 Alveolar Capillary Dysplasia: A Spectrum of Clinicopathologic Manifestations

Margaux Canevari[1], Constance DiAngelo[2], Holly Babcock[3], Geovanny Perez[3], Christopher Rossi[4]
[1]Walter Reed National Military Medical Center, Rockville, MD, [2]Washington, DC, [3]Children's National Medical Center, Washington, DC, [4]Arlington, VA

Disclosures: Margaux Canevari: None; Holly Babcock: None; Geovanny Perez: None

Background: Alveolar capillary dysplasia with misalignment of pulmonary veins (ACD) is considered to be, without transplant, a uniformly fatal disease. The lethality is largely due to the reduced gas exchange caused by the disordered architecture of the respiratory unit. Heterozygous mutations in *FOXF1* are associated with ACD. With the increased availability of genetic testing, there is a newer understanding that the disease includes variable expressivity and a wider spectrum of severity. We report two cases of ACD, including one with a heterozygous, *de novo FOXF1* gene variant not previously reported in individuals with disease.

Design: Two cases were received and reviewed by two pathologists. Clinical information and genetic testing reports were obtained and reviewed by the pulmonology, genetics, and/or pathology teams.

Results: Both patients were born at full term following uncomplicated pregnancies and were initially stable after delivery. They acutely decompensated in the nursery requiring NICU admission for respiratory support. The male patient required central ECMO placement, during which time a lung biopsy was performed that revealed findings typical for ACD. His genetic testing was unrevealing including a chromosome microarray and Next Generation sequencing panel of 48 genes including *FOXF1*. He died at 17 days of life. The female patient had episodic desaturation events with occasional stretches of being weaned to room air. Cardiac catheterization showed a patent foramen ovale and severe idiopathic pulmonary hypertension at 1 month of age. Genetic testing revealed a heterozygous variant of unknown significance in *FOXF1* (c.325_333delCTACCCAAG; p.Leu109_Lys111del). Parental testing was completed confirming the variant to be *de novo*, increasing the likelihood of pathogenicity. A biopsy was performed revealing more mature alveolar development and patchier alveolar septal thickening than typically seen in ACD cases. Given the patient's relatively stable status and age, she underwent evaluation for lung transplant, but ultimately died at 6 months of age from complications of a respiratory infection.

Conclusions: These two cases further illustrate the spectrum of clinical, pathologic, and genetic manifestations that can be seen in ACD. Additionally, these cases demonstrate our limitation of understanding of the possible molecular etiologies. We also report the clinical manifestations and pathologic findings of a patient with a previously unreported *de novo FOXF1* variant.

1850 Utility of CSF Cytokines to Discriminate CNS Diseases in Pediatric Patients

Timothy Chao[1], Ana Maria Cardenas[2], Danielle Fortuna[3], Rhonda Kean[1], Douglas Hooper[1], Mark Curtis[1]
[1]Thomas Jefferson University Hospital, Philadelphia, PA, [2]BD, Sparks, MD, [3]Hospital of the University of Pennsylvania, Philadelphia, PA

Disclosures: Timothy Chao: None; Ana Maria Cardenas: *Employee*, BD; *Employee*, Thrive Early Detection; Danielle Fortuna: None; Rhonda Kean: None; Douglas Hooper: None; Mark Curtis: None

Background: Rapid characterization of CNS diseases in pediatric patients is necessary for initiating timely and proper care. However, determining if the CNS is involved and identifying the type of CNS disease are often difficult in the acute setting. Novel diagnostic approaches quantifying the immune response elicited by different CNS disorders may contribute to the rapid determination of CNS disease type. Here we quantify and identify CSF cytokines useful in distinguishing pediatrics patient with CNS bacterial infections, viral infections, primary tumors, autoimmune diseases, and systemic disease without CNS involvement.

Design: We quantified 41 CSF cytokines in pediatric patients (ages 11 days-14years) with CNS bacterial infections (n = 14), viral infections (n = 20), autoimmune diseases (n = 5), and primary tumors (n = 9), with 12 control samples without CNS involvement. Traditional CSF values (protein, glucose, and white blood cell counts) were also measured. Linear discriminant analysis (LDA) was used to demonstrate if CSF cytokines can be used to cluster samples by their CNS disease types. The Kruskal-Wallis and post-hoc Mann-Whitney tests were used to determine significant differences. Unbiased random forest machine learning then selected cytokines with the highest ability to discriminate the CNS disease classes. Finally, we compared the accuracy of a decision tree built with the selected cytokines to a tree built with routine CSF values.

Results: LDA showed that CSF cytokines can distinctly cluster samples by CNS disease types. Indeed, 39 of 41 cytokines showed significant differences among the CNS disease classes. An unbiased algorithm then selected 7 cytokines (IL17A, IL12p40, TNFA, IL1A, IP10, IL1RA, and MDC) with the highest discriminatory power among the different CNS disease types. Finally, a decision tree with these cytokines significantly outperformed a tree using routine CSF values (accuracy 86.7% vs. 76.7%).

Conclusions: We demonstrate that CNS disease types in pediatric patients have distinct CSF cytokine profiles. A panel of 7 cytokines with the highest potential to distinguish the CNS disease types was unbiasedly selected. A decision tree using these cytokines outperforms a decision tree built using only routine CSF values. Our work highlights the utility of CSF cytokine analysis to guide clinical decisions by identifying the likely class of CNS disease.

1851 Evaluation of the Response to Oral Budesonide by the New Histology Scoring System Developed for Eosinophilic Esophagitis Patients

Peyman Dinarvand[1], Odianosen Eigbire-molen[2], Miguel Guzman[1], Danielle Carpenter[3]
[1]Saint Louis University, St. Louis, MO, [2]Department of Pathology, Saint Louis University, St. Louis, MO, [3]St. Louis University School of Medicine, St. Louis, MO

Disclosures: Peyman Dinarvand: None; Odianosen Eigbire-molen: None; Miguel Guzman: None; Danielle Carpenter: None

Background: Most patients with eosinophilic esophagitis (EoE) respond to oral budesonide (BUD) (usually after failure in dietary approaches and proton pump inhibitor use) as demonstrated by a decrease in eosinophil counts. Histologic predictors and changes during response to BUD are poorly understood and not well-studied. In this study, we use a newly developed histologic scoring system to identify changes that predict response to BUD in patients with EoE.

Design: A single institution retrospective review identified 38 pediatric patients (average age of 7 years) with EoE (≥15 intraepithelial eosinophils/high power field) who had failed treatment on proton pump inhibitors, subsequently received BUD, and had a minimum of three additional biopsies at 6 month follow-up intervals (210 biopsies) after starting BUD (T1: first biopsy, T2: second biopsy, T3: third biopsy). Sixteen randomly selected patients (30 biopsies), without EoE and with normal endoscopic and histological findings, were included as controls. Eight features in proximal and distal esophagus- eosinophil inflammation (EI), basal zone hyperplasia (BZH), eosinophil abscess (EA), eosinophil surface layering (SL), dilated intercellular spaces (DIS), surface epithelial alteration (SEA), dyskeratotic epithelial cells (DEC), and lamina propria fibrosis (LPF)- were scored (by two pathologists in a blinded fashion) based on severity (grade) and extent (stage) using a 4-point scale (0, normal; 3, maximum change).

Results: Seven out of the eight features showed a significant decrease in grade and stage during treatment. In treated patients, median grade and stage scores significantly dropped for BZH, SEA, and EI at T2 in the proximal esophagus only (Figure 1). Both the proximal and distal esophagus showed a significant decrease in other variables (except LPF) at T3 (Figure 1). Importantly, median stage scores of treated individuals at T3 (last) time point with 0 eosinophils/high power field (hpf) still showed LPF, BZH, and DIS in both proximal and distal esophagus (Figure 1). Additionally, scores for BZH, DIS, and LPF were significantly higher at T3 of treated group versus controls in both proximal and distal esophagus.

Figure 1 – 1851

Grade scores	Distal				Proximal			
	First Biopsy (T1)	Second Biopsy (T2)	Third Biopsy (T3)	P-value	First Biopsy (T1)	Second Biopsy (T2)	Third Biopsy (T3)	P-value
EI	2(2-3)	2(1-3)	1(0-2)	0.31	3(2-3)	2(1-2)	1(0-1)	**0.0008***
BZH	2(2-2)	2(1-2)	1(1-2)	1.0	2(2-2.5)	2(1-2)	1(0-2)	**0.02***
DIS	3(2-3)	2(1-3)	2(1-2)	0.15	2(2-3)	2(1-2.5)	1(1-2)	0.19
LPF	1(1-2)	1(0.75-2.0)	1(1-1)	1.0	1(1-2)	1(1-2)	1(0.75-1)	1.0
EA	0(0-1)	0(0-1)	0(0-0)	1.0	1(0-2)	0(0-1)	0(0-0)	0.07
SL	1(0-2)	0(0-1)	0(0-0)	0.52	2(0-2)	0(0-1)	0(0-0)	0.027*
SEA	1(0-2)	0(0-1)	0(0-0)	0.49	1(1-2)	0(0-1)	0(0-0)	**0.035***
DEC	0(0-1)	0(0-0)	0(0-0)	1.0	0(0-0.5)	0(0-0)	0(0-0)	1.0
Stage scores	**Distal**				**Proximal**			
	First Biopsy (T1)	Second Biopsy (T2)	Third Biopsy (T3)	P-value	First Biopsy (T1)	Second Biopsy (T2)	Third Biopsy (T3)	P-value
EI	2(1-2)	1(1-2)	0(0-1)	0.25	2(1-2)	1(0-2)	0(0-1)	**0.009***
BZH	2(2-2)	2(1-2)	1(1-1)	1.0	2(2-2)	2(1-2)	1(0-1)	**0.025***
DIS	2(2-3)	2(1-2)	1(1-2)	0.33	2(2-2.5)	2(1-2)	1(1-2)	0.27
LPF	1(1-2)	1(0.5-1)	1(1-1)	1.0	1(1-2)	1(1-1)	1(0.75-1)	0.72
EA	0(0-2)	0(0-1)	0(0-0)	1.0	1(0-2)	0(0-1)	0(0-0)	0.11
SL	1(0-2)	0(0-1)	0(0-0)	0.95	1(0-2)	0(0-1)	0(0-0)	0.057
SEA	1(0-2)	0(0-1)	0(0-0)	0.47	1(1-2)	0(0-1)	0(0-0)	**0.027***
DEC	0(0-1)	0(0-0)	0(0-0)	1.0	0(0-0.5)	0(0-0)	0(0-0)	0.92

Figure 1: Grade and Stage scores (median and interquartile range) for EoE histologic features.
P values - Comparison of First biopsy (**T1**) and Second biopsy (**T2**) scores by Wilcoxon signed rank test.
*P ≤ 0.05 (after Bonferroni adjustment for multiple testing).

Conclusions: BZH, SEA, and EI in proximal esophagus respond to BUD earlier and potentially can be used as predictors of response to treatment in EoE patients. Presence of LPF, BZH, and DIS in treated individuals with 0 eosinophils/hpf could justify continuous clinical symptoms in some treated patients with 0 eosinophils.

1852 The Value of Quantitative Assessment of Ganglion Cells at the Proximal Resection Margin After Colorectal Pull Through in Hirschsprung's Disease

Saleh Fadel[1], Marco Law[2], Victoria Madge[3], Adrian Chan[4], Deepti Reddy[5], Ahmed Nasr[5], Joseph de Nanassy[6], Dina El Demellawy[7]
[1]University of Ottawa/The Ottawa Hospital, Ottawa, ON, [2]The University of British Columbia, Vancouver, BC, [3]Carleton University, Montreal, ON, [4]Carleton University, Ottawa, ON, [5]Children's Hospital of Eastern Ontario, Ottawa, ON, [6]Children Hospital of Eastern Ontario, Ottawa, ON, [7]Ottawa, ON

Disclosures: Saleh Fadel: None; Marco Law: None; Victoria Madge: None; Adrian Chan: None; Deepti Reddy: None

Background: Hirschsprung's disease (HD) is a congenital condition characterized by the absence of parasympathetic intrinsic ganglion cells of the enteric nervous system in the large intestine. It leads to an intestinal obstruction that can be life-threatening. HD is diagnosed by rectal suction biopsy. The standard treatment is a pull-through surgery where the aganglionic segment is resected and the normal ganglionic segment is re-anastomosed to the anus. Some patients' symptoms persist despite successful surgery and they may require life-long treatment measures or a pull-through redo which is much more technically difficult. It is not yet known what factors contribute to this outcome. In this study, we investigated whether the amount of ganglion cells at the proximal resection margin could predict post-operative complications.

Design: We performed a retrospective analysis of all cases of HD at the Children Hospital of Eastern Ontario (CHEO) from 1997-2016. 26 cases were included in the study. The data collected included demographics, surgical parameters, pathological parameters, HD-related outcomes, and surgery-related complications. The number of ganglion cells were counted on HPS-stained and Calretinin-stained slides. A computer program was developed for automatic quantification of ganglions and was used for Calretnin-stained slides.

Results: The average number of ganglion cells per plexus at the proximal margin and the number of ganglion cells per muscularis propria surface area did not predict HD-related patient outcome after successful surgery using any of the 3 counting methods (HPS manual p=0.92 for both; Calretinin manual p=0.22 for both; digital p=0.83 and p=0.53, respectively). The length of ganglionic segment in the resected margin was correlated with patient outcome (p<0.02). Those with ganglionic segments shorter than 7.7 cm (as estimated by the Youden index) were less likely to have any type of complication.

Conclusions: There is no added value in counting the ganglions of the myenteric plexus at the proximal resection end in HD patients as they do not predict the chance of developing complications. Our study suggests that resecting a longer ganglionic segments (>7.7 cm) correlates with higher risk of complications, and so it may be more beneficial to resect a shorter ganglionic segment above the transitional zone in a pull-through procedure for HD.

1853 Novel Clinicopathological Insights in Racial and Disease Variance in Pediatric Eosinophilic Esophagitis Patients

Karina Furlan[1], Joanna Solarewicz[1], Prih Rohra[1], Shriram Jakate[1]
[1]*Rush University Medical Center, Chicago, IL*

Disclosures: Karina Furlan: None; Joanna Solarewicz: None; Prih Rohra: None; Shriram Jakate: None

Background: Eosinophilic esophagitis (EoE) is a chronic immune/antigen-mediated, inflammatory esophageal disease with an estimated overall prevalence of 25.9/100,000 in the adult and pediatric population in the USA. The diagnostic criteria are well established and include symptoms related to esophageal dysfunction, a spectrum of endoscopic abnormalities and histological changes with increase in eosinophils (>15/HPF). The racial and gender variation of EoE patients have shown to directly affect the prevalence of symptoms and endoscopic findings in different groups. We conducted a clinicopathological study to investigate racial and disease variance in the pediatric population of a single tertiary institution.

Design: A retrospective study was performed including pediatric patients with clinical and biopsy proven EoE in the last 20 years (1999-2019). The final outcome was to evaluate and compare clinical, endoscopic and histologic variances of the disease in different races.The patients were divided in three racial groups - Caucasian, African-American and others (Hispanic or Asiatic). Data were collated and analyzed using statistical software (SPSS, version 21, IBM, Armonk, NY).

Results: A total of 172 pediatric patients (<18 years of age, 73% males, 27% females, median age 10) were included. The patients were divided in three racial groups - Caucasian, African-American and others (Hispanic or Asiatic). African American patients had a higher prevalence of failure to thrive in comparison with other groups (p<0.01), they presented with a normal initial endoscopy examination in 46% of the cases, however complications as stricture and narrowing were significantly more prevalent in this group when compared with the other racial groups (<0.01). The number of eosinophils in tissue biopsy was comparable between the different racial groups, however patients younger than 12 years old presented with a significantly higher number of eosinophils (>25/HPF) (p<0.01).

Race	White	Black	Others
Frequency n (%)	120 (69.77)	43 (25)	9 (5.23)
Gender - Female n (%)	32 (26.6)	11 (25.5)	1 (11.12)
Gender - Male n (%)	88 (73.3)	32 (74.4)	8 (88.88)
Age at diagnosis (median range)	12 / 1-19 yo	6 / 1-19 yo	3 1-18 yo
Years of disease (median/range)	9.5 / 1-17	6 / 1-18	6 / 1-12

Figure 1 - 1853

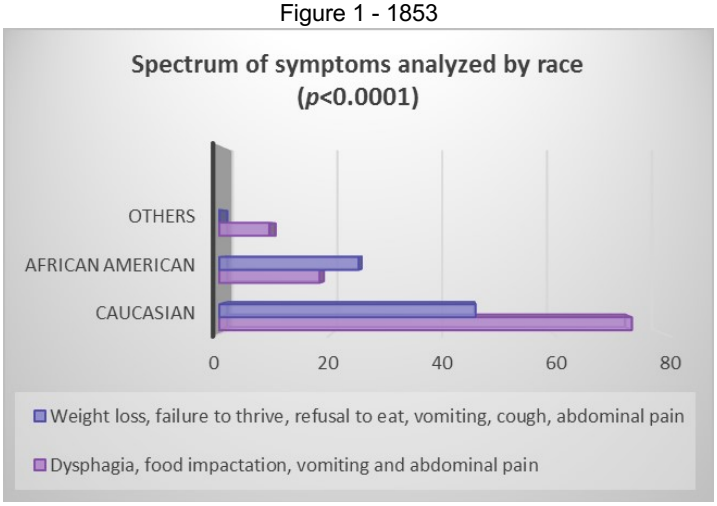

Conclusions: African American patients display a distinctive subtype of EoE characterized by younger age of presentation (mean age of 6), higher prevalence of failure to thrive, more common normal endoscopy and greater occurrence of strictures. While histological findings are similar across racial groups, the younger patients (<12 yrs) overall have markedly increased eosinophils (>25/HPF). Larger prospective studies are required to investigate these variations in EoE presentation in both pediatric and adult populations.

1854 Immunohistochemistry Panels to Help Understand Differentiation and Maturation of Mesonephros and Metanephros

Alia Gupta[1], Jacqueline Macknis[2], Ping Zhang[3]
[1]Troy, MI, [2]William Beaumont Hospital, Royal Oak, MI, [3]William Beaumont Hospital, Birmingham, MI

Disclosures: Alia Gupta: None; Jacqueline Macknis: None; Ping Zhang: None

Background: Mesonephros (MS) acts as embryonic renal tissue transiently. It forms metanephric duct and finally differentiates into mature kidneys. MS is also a source of somatic cells in the male gonad, versus ovarian tissue which has paramesonephric origin. Histology of MS and metanephros (MT) is partially established. However, demonstration of differentiation and maturation of these embryonal structures has not been studied extensively, especially using immunohistochemical (IHC) staining methods. Therefore, IHC staining was employed in this study to compare the expression patterns of MS and MT in an attempt to better understand its differentiation and maturation.

Design: 4 MS (6 to 10 weeks) and 10 MT (10 to 36 weeks) were included in the study and paraffin embedded tissue with MS and/ or MT was sectioned and stained with two panels of antibodies; panel targeting stem cell/ progenitor cell population, including PAX8, OCT3/4 and CD133 and panel targeting growth factors and maturation/ mesenchymal markers, including mTOR, downstream signal p70S6K, WT-1 and vimentin. Light microscopy for each stain was evaluated and scored from negative (0) to positive (1+ to 3+; weak/fine to strong/granular staining).

Results: PAX8 was expressed in glomeruli and renal tubules at all stages of MT development. OCT3/4 was absent in all renal tissues. However, OCT3/4 was expressed in the gonadal portion of a 10 week transforming MS (phenotypically male) with negative for PAX8 staining (Figure 1). CD133 was negative in MS and MT glomeruli. MS and early MT showed extensive expression of mTOR, p70S6K, WT-1 and vimentin in glomeruli and interstitium. Whereas, from 17 to 36 weeks of gestation, there was a graduated weakening of staining of these markers in the interstitium of MT, which was replaced by expanding renal tubules (negative for WT-1 and vimentin). With maturation, the glomeruli showed fading of mTOR and p70S6K staining and retained WT-1 and vimentin immunoreactivity, even in late stages of MS development (fetal kidneys).

Figure 1 - 1854

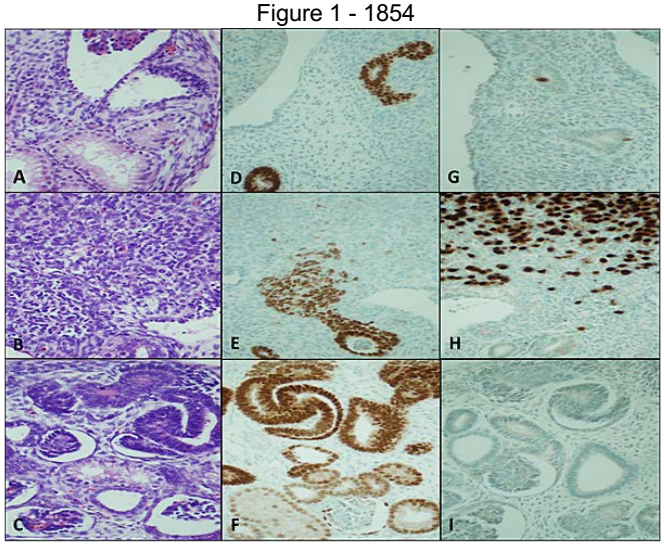

Figure 1. A-I: Higher power view (400X; H&E) showing early mesonephros (A), early gonad (B) and glomerulus with renal tubules in late mesonephros (C). PAX 8 expression in mesonephros (positive in scattered renal tubules; D), negative in early gonad (positive in adjacent tubules; E) and positive in early metanephros (both primordial glomeruli and renal tubules; F). OCT3/4 expression in late mesonephros (focally positive in renal tubules; G), diffusely positive in early gonad (H) but negative in early metanephros (both primordial glomeruli and renal tubules; I).

Conclusions: OCT3/4 was expressed in gonadal tissue (most likely male fetus) that lacked PAX8 staining. This might help explain why testicular neoplasms show OCT3/4 staining whereas PAX8 is usually positive in renal and ovarian epithelial tumors. Mesenchymal to epithelial transformation in MT is characterized by graduated silencing of growth factors and disappearance of WT-1 and vimentin in the interstitial tissue of kidney.

1855 Histologic Features of Response to Larotrectinib in Infantile Fibrosarcoma

Shannon Kelley[1], Veena Rajaram[1], Theodore Laetsch[1], Dinesh Rakheja[1]
[1]*University of Texas Southwestern Medical Center, Dallas, TX*

Disclosures: Shannon Kelley: None; Veena Rajaram: None; Theodore Laetsch: *Consultant*, Bayer; *Grant or Research Support*, Bayer; Dinesh Rakheja: None

Background: Infantile fibrosarcoma (IF) is characterized by *ETV6-NTRK3* or less commonly *LMNA-NTRK1* fusion. Till recently, the mainstay of treatment was surgical resection with adjuvant or neo-adjuvant chemotherapy with vincristine, actinomycin, and cyclophosphamide (VAC). However, some tumors are refractory. Recently, TRK inhibitors have been developed with Larotrectinib approved by the FDA for tumors with *NTRK* fusions. The histologic features of IF treated with larotrectinib have not previously been described.

Design: Between 2015 and 2019, 3 patients with IF were treated with Larotrectinib followed by resection at our institution. In each case, the initial biopsy showed characteristic IF histology and *ETV6-NTRK3* fusion. Histologic examination of the resected specimen was performed.

Results: Figure 1 provides an example of the pre-treatment histology noted in patient C. Clinical response was noted in each patient. Histologic examination showed residual IF in patients A and B and no residual tumor in patient C (Figure 2). In each case, there was hypocellular fibrocollagenous tissue with abundant thin and thick-walled blood vessels. Residual tumor cells in patients A and B were slender compared to the plumper tumor cells in the diagnostic biopsy. In patient C, there was persistent *ETV6-NTRK3* fusion despite negative histology. Residual tumor extended to resection margins in patients A and B, and the tumor bed extended to resection margin in patient C.

Patient	Gender	Lesional Location	ETV6-NTRK3 fusion	Initial treatment	Length of treatment with Larotrectinib	Residual histologic tumor	Persistent fusion post treatment
A	Boy	Left foot	Present	Propanolol	1 month	Yes	Not assessed
B	Boy	Gluteal mass	Present	Vincristine and Actinomycin	4 months	Yes	Not assessed
C	Boy	Left forearm	Present	VAC	2.5 years	No	Yes

Figure 1 - 1855

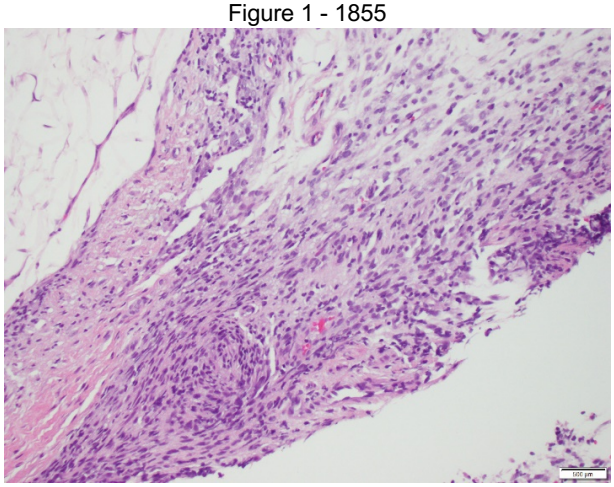

Figure 2 - 1855

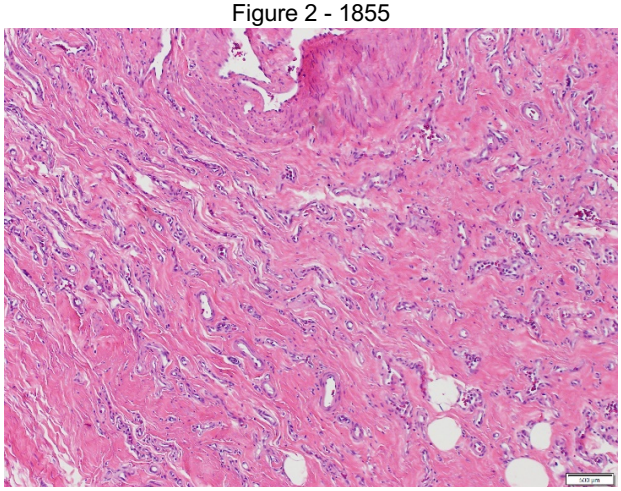

Conclusions: We had a unique opportunity to study the effect of larotrectinib for various durations on IF. Residual IF was noted histologically after 1 and 4 months of treatment but was not noted after 2.5 years of treatment. However, even after 2.5 years, there was persistent *ETV6-NTRK3* fusion. Residual IF cells appeared slender and more “mature”, suggesting that potential residual IF cells in the 3rd case were completely mature fibroblasts not distinguishable as tumor cells. The patients continue to be clinically followed, which will reveal whether there is a risk for recurrence or metastasis.

1856 Pediatric Autoimmune Metaplastic Atrophic Gastritis

Ozlem Kulak[1], Jason Park[2]
[1]UT Southwestern Medical Center, Dallas, TX, [2]Children's Medical Center Dallas, Dallas, TX

Disclosures: Ozlem Kulak: None; Jason Park: None

Background: Autoimmune metaplastic atrophic gastritis (AMAG) is an underrecognized entity which in adult studies has been reported with a frequency as high as 4% in select patient populations. There have been few descriptions of autoimmune gastritis in pediatric patients.

Design: In this retrospective study of a single tertiary care pediatric center, we identified all gastric biopsies described as autoimmune gastritis from 2011-2019 using the search terms of “autoimmune gastritis”, “autoimmune metaplastic atrophic gastritis”, “AMAG” or “atrophic gastritis”. All cases had body-predominant inflammation with enterochromaffin-like (ECL) cell hyperplasia. All cases were negative for H. pylori.

Results: Twenty-four patients met the criteria for AMAG. The median age at first biopsy was 11.5 years, and 15 patients were female. The most common self-identified race was Hispanic (n=13). The most common clinical indications for endoscopic evaluation were anemia (n=19), abdominal pain (n=11), gastrointestinal bleeding (n=6), anemia (n=6), and failure to thrive/weight loss (n=6), and vomiting (n=6). In addition to body-predominant inflammation with ECL hyperplasia, antral inflammation (n=6) and intestinal metaplasia (n=3) were identified. Positive laboratory findings included (of patients tested): anti-parietal cell antibodies (6 of 13); serum gastrin (6 of 11), iron deficiency (4 of 13), antinuclear antibody (3 of 12), thyroid peroxidase (2 of 2), rheumatoid Factor (1 of 2); vitamin B12 deficiency (1 of 16). Extra-gastric diseases were identified in 13 of 24 patients, including CHARGE syndrome, Type 1 diabetes, hypothyroidism, common variable immunodeficiency, organ transplantation, autoimmune hepatitis, juvenile arthritis, and glycogen storage disease. Of the patients with clinical follow-up (n=16) (median 23 months; range 1-68 months), 50% were symptomatic with abdominal pain, nausea/emesis or poor weight gain.

Conclusions: We have identified 24 cases of AMAG over a nine-year time period. Most cases had the classic histologic definition; however, antral inflammation was frequently identified. Autoimmune gastritis should be in the differential for body-specific gastritis of pediatric patients.

1857 Ocular Tumors of Childhood: Presentation of Three Uncommon Cases

Gabriela Lamas[1], Ezequiel Nespoli[2], Maria Galluzzo Mutti[2], Maria Davila[3], Fabiana Lubieniecki[4]
[1]Buenos Aires, Argentina, [2]Hospital Garrahan, Buenos Aires, Argentina, [3]Hospital Britanico de Buenos Aires, Ciudad de Buenos Aires, Argentina, [4]Hospital de Pediatria J.P.Garrahan, Buenos Aires, Argentina

Disclosures: Gabriela Lamas: None; Ezequiel Nespoli: None; Maria Galluzzo Mutti: None; Maria Davila: None; Fabiana Lubieniecki: None

Background: Because of its highly complex structures, tumors that originate from the eye globe are varied. However, these tumors are rare in childhood, being the retinoblastoma the most common pediatric intraocular neoplasm, accounts for 3% of all pediatric tumors. Nevertheless, there are other entities that pose a challenge at the time of making the clinical and histopathological diagnosis.

Design: Here we present three cases of intraocular tumors in pediatric patients that were enucleated, seen at a single institution.

Results: Case 1: A 9-year-old girl who started at 7 years of age with a lesion in the right eye located in the juxtapapillary nasal retina. On macroscopy, a white-yellowish mass of 1.1 x 0.8 cm was seen. Histology showed a tumor consisting vascular structures and stromal cells with clear cytoplasm. On immunohistochemistry, vascular structures were positive for CD31 and CD34 and the stromal cells were positive for inhibin, NSE, and vimentin. Diagnosis: HEMANGIOBLASTOMA. Case 2: An 8-year-old boy with a subretinal tumor in the supra-macular area of the left eye. Macroscopy showed a whitish 1 x 1 cm tumor adjacent to the optic nerve. Microscopy revealed a tumor composed of spindle cells with hyperchromatic nuclei with moderate pleomorphism and eosinophilic-to-clear cytoplasm, arranged in bundles. Interspersed cuboidal cells arranged in nests and tubules were observed. Some mitosis were found. The cells were positive for HHF35, SMA and CK18. Groups of cuboidal cell were positive for EMA, HMB45, MELAN A and synaptophysin. Diagnosis: MESECTODERMAL LEIOMYOMA. Case 3: A girl of one month of life, with progressive proptosis since birth. Macroscopy showed a solid, heterogeneous tumor, involving the entire eyeball. Microscopy showed a tumor with cells with vesicular nuclei, prominent nucleoli, and abundant eosinophilic cytoplasm in some of them. There was abundant mitosis and extensive necrosis. Immunohistochemistry showed loss of INI1 protein and positivity for EMA, CKAE1/AE3, and synaptophysin. Diagnosis: RHABDOID TUMOR.

Conclusions: These tumors have been reported in the literature as isolated cases, of which the rhabdoid tumor is the most exceptional. In the registry of our pediatric reference center, these are the only documented cases. The collection of data on ocular tumors other than retinoblastoma in children will contribute both to a better clinical management and histopathological diagnosis of these cases.

1858 Skin Biopsies from Aicardi-Goutièrez Patients Show Mutation-Specific Interferon-Induced Immunophenotype

Luisa Lorenzi[1], Jessica Galli[2], Rosalba Ferraro[3], Donatella Vairo[1], Paolo Incardona[4], Mattia Bugatti[5], Debora Bresciani[6], Andrea Bernardelli[7], Simona Orcesi[8], Giulio Gualdi[9], Elisa Fazzi[1], Silvia Giliani[1], Facchetti Fabio[10]
[1]University of Brescia, Brescia, Italy, [2]Department of Clinical and Experimental Sciences, University of Brescia; Child Neurology and Psychiatry Unit, ASST Spedali Civili of Brescia, Brescia, Italy, [3]Nocivelli Institute of Molecular Medicine, University of Brescia, Brescia, Italy, [4]ASST Spedali Civili, Brescia, Italy, [5]Spedali Civili di Brescia, Brescia, Italy, [6]Pathology Unit ASST Spedali Civili di Brescia, Lumezzane, BS, Italy, [7]University of Verona, Verona, VR, Italy, [8]S.C. Child Neurology and Psychiatry Unit, Fondazione Istituto Neurologico, Pavia, Italy, [9]Dermatology Unit, ASST Spedali Civili di Brescia, University of Brescia, Brescia, Italy, [10]Pathology Unit, University of Brescia, Brescia, Italy

Disclosures: Luisa Lorenzi: None; Jessica Galli: None; Rosalba Ferraro: None; Donatella Vairo: None; Paolo Incardona: None; Mattia Bugatti: None; Debora Bresciani: None; Andrea Bernardelli: None; Simona Orcesi: None; Giulio Gualdi: None; Elisa Fazzi: None; Silvia Giliani: None; Facchetti Fabio: None

Background: Aicardi-Goutières Syndrome(AGS)is a rare genetic interferonpathy with onset in the first year of life, characterized by severe neurological symptoms caused by germline mutations on *TREX1,RNASEH2A-2B-2C,SAMHD1,ADAR1* or *IFIH1* leading to uncontrolled production of Interferon(IFN)-α whose levels increase in cerebrospinal fluid and serum. IFN-signature on circulating leukocytes (IFN-S) was recently proposed as screening tool in AGS diagnosis. Skin lesions, chilblain-like, may occur in AGS-patients, in particular in those carrying *TREX1* and *IFIH1* mutations, however, little data is available on cutaneous histological findings in these patients.

Design: Biopsies were performed on AGS patients on both normal and lesional skin. Formalin fixed and paraffin embedded tissue was used for morphological evaluation and for immunohistochemistry (IHC). Interferon (IFN) related proteins MxA, phospho-STAT1 and ISG15 were applied and semi-quantitative score performed on the epidermis based on number of positive cells (score 0-4). Plasmocytoid dendritic cells (PDC) were detected by BDCA2/CD303 or CD123 staining.

Results: Ten patients were enrolled in the study (Table). Normal skin was biopsied in all, chilblain of the calcaneus and erythematous lesion of the knee were performed in P#1 and P#4. On morphology, normal skin biopsies showed unremarkable findings; lesional biopsy of P#1 showed abundant perivascular lymphocytic infiltrate and occasional PDC; in P#4 basal membrane was thickened, abundant lymphocytic infiltrate perivascular and perieccrine and intravascular trombi were found. IFN-related proteins were validated on skin from healthy subjects (negative) and from Lupus patients (positive control). In AGS, epidermal expression of IFN-related proteins was detected both in normal and lesional biopsies of patients carrying mutations on *IFIH1*, *TREX1* and *ADAR1* while being negative or low in those with mutations on *RNASEH2B*. Notably, despite high expression of IFN-induced proteins, PDCs were absent or scarce in AGS skin and never at the dermo-epidermal junction where they typically localize in Lupus.

Pt #	Female/Male	Age in years	AGS subtype	Mutated gene	Skin biopsy	MxA	pSTAT1	ISG15	IFN signature
1	M	5	AGS1	TREX1	normal	4	2	na	positive
1	M	5	AGS1	TREX1	lesional	4	1		
2	F	10	AGS2	RNASEH2B	normal	0	2	0	na
3	M	15	AGS2	RNASEH2B	normal	0	0	0	positive
4	M	11	AGS7	IFIH1	normal	4	4	4	positive
4	M	11	AGS7	IFIH1	lesional	4	4	na	positive
5	M	10	AGS7	IFIH1	normal	4	4	4	positive
6	F	3	AGS6	ADAR1	normal	4	1	2	positive
7	M	13	AGS2	RNASEH2B	normal	0	1	2	negative
8	M	5	AGS2	RNASEH2B	normal	0	0	0	positive
9	M	3	AGS7	IFH1	normal	4	0	1	positive
10	F	2	AGS2	RNASEH2B	normal	0	1	0	positive

Figure 1 - 1858

Pt #5 *IFIH1*-mutated (AGS7)

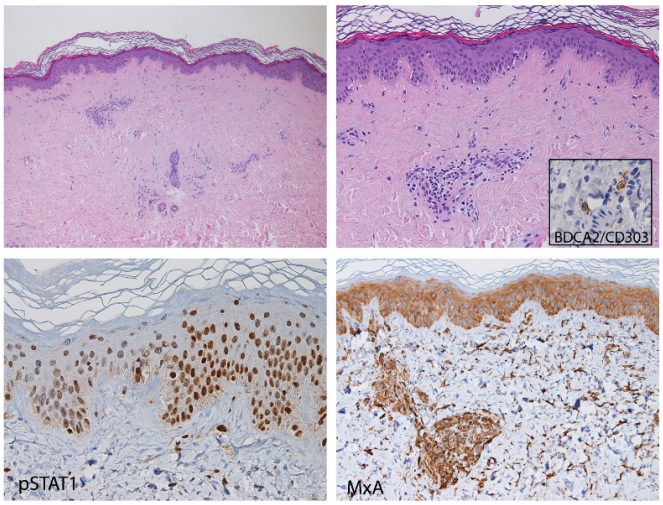

Figure 2 - 1858

Pt #2 RNASEH2A-mutated (AGS2)

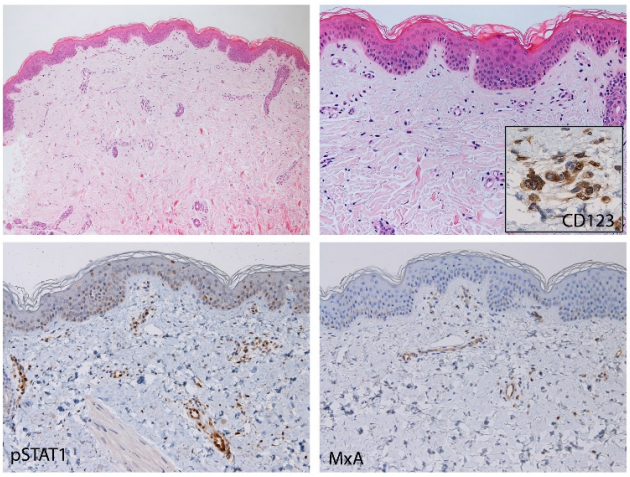

Conclusions: Irrespectively from PDC infiltration, “Cutaneous IFN-signature” by IHC is positive in all AGS patients but those with *RNASEH2B* mutations, showing higher mutation-specificity than IFN-S. Skin biopsy may convey additional information in the diagnostic workout of AGS and offer new pathobiological information on this rare and severe disease.

1859 Granular Cell Tumor of the Esophagus in Children: Report of 8 Cases

Faizan Malik[1], Anas Bernieh[2], Amin Hayee[3], Siraj El Jamal[4], Ali Saad[5]

[1]University of Tennessee Health Science Center, Memphis, TN, [2]Cincinnati Children's Hospital Medical Center, Cincinnati, OH, [3]University of Miami/Jackson Memorial Hospital, Miami, FL, [4]Icahn School of Medicine at Mount Sinai, New York, NY, [5]University of Miami Miller School of Medicine, Miami, FL

Disclosures: Faizan Malik: None; Anas Bernieh: None; Amin Hayee: None; Siraj El Jamal: None; Ali Saad: None

Background: Granular cell tumor (GCT) is considered a benign tumor of Schwannian origin and commonly involves the soft tissue. GCT of the esophagus is rare with only 6 reported cases in children; and only 4 in association with eosinophilic esophagitis (EoE). We report the largest series of pediatric esophageal GCT.

Design: The files of multiple children’s hospitals were searched for pediatric patients with GCT of the esophagus. Review of histologic slides and immunohistochemical studies for S100, CD68 and SOX10 was performed along with correlation with clinical, endoscopic and follow-up data procured from the medical records.

Results: 8 pediatric patients with GCT of the esophagus were identified. There were 6 males and 2 females. The median age was 5.5 years (range 3-14 years). Patients underwent esophagogastroduodenoscopy (EGD) for the following reasons: follow-up for EoE (n=3), dysphagia (n=2), epigastric pain (n=1), gastroesophageal reflux (GERD) (n=1), and nonspecific abdominal pain (n=1). By EGD, all tumors had a well-circumscribed, firm, and nodular appearance with luminal protrusion resembling a sessile polyp. The overlying mucosa was unremarkable in all cases. In all patients, gross total excision was performed by removing the tumor in multiple biopsies. The median size of the tumor was 4.75 mm (range 3-8.5 mm) with the largest tumors (7 and 8.5 mm, respectively) in the two patients presenting with dysphagia. Histologic evaluation showed tumor cells with bland nuclei and large pink finely granular cytoplasm. The tumor cells were mostly arranged in sheets with some trabeculae, particularly at the periphery. The borders were mostly well-demarcated with foci of infiltrative growth. Atypical cytological features or mitoses were absent. All cases showed tumor cell positivity for S100, CD68, and SOX10. Follow-up (median: 1.5 years; range 0.5-3 years) showed no recurrence on EGD (n=6), whereas 2 patients without EGD at follow-up remained symptom-free after removal.

Conclusions: We report herein the largest series of pediatric esophageal GCT. Our findings also suggest a coincidental association of GCT with EoE. Except when a certain size is reached, these tumors are usually discovered incidentally. EGD findings are characteristic and removal by biopsy is both diagnostic and therapeutic. Biopsy is also recommended to rule out other esophageal tumors of childhood.

1860 Clinicopathologic Comparison of Autoimmune Antibody Serology in Pediatric Patients with Non-Alcoholic Fatty Liver Disease and Autoimmune Hepatitis

Rachel Mariani[1], Dustin Bunch[2], Shamlal Mangray[3], Bonita Fung[2]
[1]Nationwide Children's Hospital - The Ohio State University, Columbus, OH, [2]Nationwide Children's Hospital, Columbus, OH, [3]Nationwide Children's Hospital, Providence, RI

Disclosures: Rachel Mariani: None; Dustin Bunch: None; Shamlal Mangray: None; Bonita Fung: None

Background: Serologic tests for autoantibodies such as antinuclear antibody (ANA) or antismooth muscle antibody (ASMA) are often a component of comprehensive laboratory testing for the work-up of pediatric patients with elevated liver function tests. Positive ANA serology (titers > or = 1:80) has been reported in some adult and pediatric patients with liver biopsy findings consistent with non-alcoholic fatty liver disease (NAFLD) and no features of autoimmune hepatitis (AIH), i.e., no significant interface activity. We have also observed this trend in our clinical experience. The significance of positive autoantibodies remains unclear in pediatric NAFLD. We investigated the relationship between autoantibodies and other laboratory parameters as well as histopathologic findings in needle core biopsies in a large pediatric cohort with NAFLD and also compared this cohort to patients diagnosed with AIH.

Design: A retrospective search encompassing 2015-2018 was performed and patients with histopathologic features of NAFLD or AIH were identified. NAFLD activity score was tabulated for all NAFLD cases. Clinical and laboratory information was retrieved from the electronic medical record, which included age at diagnosis, body mass index (BMI), sex; ANA, ASMA, immunoglobulin G (IgG) titers; aspartate aminotransferase (AST), alanine aminotransferase, gamma-glutamyl transferase, and alkaline phosphatase serologic levels. Analysis of variables was performed.

Results: Results are summarized in table 1; 143 NAFLD and 20 AIH cases were identified. There was overall male predominance in the NAFLD cohort and female predominance in the AIH cohort. NAFLD patients were diagnosed at a younger age (p=0.0004) and had a higher BMI (p<0.0001) than AIH patients. AIH patients showed higher IgG titers (p=0.002) and higher peak AST levels (p<0.0001). ASMA titers correlated more strongly with a diagnosis of AIH than NAFLD (p<0.0001).

Table 1. Comparison of clinicopathologic features.

	NAFLD (n=143)	AIH (n=20)
Median Age/Range (years)*	14/5-20	16/1.9-20
M:F*	2:1	1:2.3
Mean BMI (kg/m^2)*	33.3	21.8
Mean peak AST level*	117	282
ANA titer Not done Negative 1:40 1:80 >1:80	15 patients 33 patients (25.8%) 31 patients (24.2%) 30 patients (23.4%) 34 patients (26.6%)	0 patients 2 patients (10.0%) 2 patients (10.0%) 2 patients (10.0%) 14 patients (70.0%)
ASMA titer* Not done Negative 1:20 1:40 >1:40	19 patients 79 patients (63.7%) 20 patients (16.1%) 16 patients (12.9%) 9 patients (7.3%)	0 patients 8 patients (40.0%) 2 patients (10.0%) 3 patients (15.0%) 7 patients (35.0%)
IgG median/range*	1090/140-1900	1630/703-4600
NAS score Median overall score Median Inflammatory Median steatosis Median balooning	4 1 3 0	N/A

*p<0.05

Conclusions: Despite elevated ANA titers in the majority of patients with NAFLD, features of AIH were lacking. Additionally, there was no relationship between any variables within the NAFLD group when stratifying patients based on ANA <1:80 or ≥1:80. The utility of ANA titers as part of a broad work up in the setting of elevated BMI is questionable and our data suggest that ANA titers may not be indicated unless very high levels of transaminases are encountered. This may lead to significant cost saving to patients and healthcare systems.

1861 Addition and Diagnostic Utility of GATA3 and ISL1 in the Small Blue Round Cell Tumors (SBRCT) of Infancy and Childhood in Differentiating Neuroblastoma from its Mimics

Sambit Mohanty[1], Jatin Gandhi[2], Manas Baisakh[3], Subhasini Naik[4]
[1]AMRI Hospital, Bhubaneswar, India, [2]University of Tennessee Health Science Center, Memphis, TN, [3]Apollo Hospitals, Bhubaneswar, India, [4]Prolife Diagnostics and Apollo Hospitals, Bhubaneswar, India

Disclosures: Sambit Mohanty: None; Jatin Gandhi: None; Manas Baisakh: None; Subhasini Naik: None

Background: Accurate diagnosis of a SBRCT of infancy and childhood often pose a challenge, especially in limited tissue specimen due to overlapping imaging, histopathologic, and immunohistochemical (IHC, infieldity among various lineage-associated transcription factors e.g. FLI1, TLE1, etc.) features. This is further compounded by the absence of material for molecular testing in doubtful cases considering the limited specimen. GATA3 and ISL1 have recently described as biomarkers of neuroblastic differentiation. Also, differentiating neuoblastoma from its mimics has important management and prognostic implications. This study aims at determining the diagnostic utility of GATA3 and ISL1 in differentiating neuroblastoma from its morphologic mimics.

Design: We tested GATA3 and ISL1 expression in 61 SBRCT of the infancy and childhood. The tumor specimens included 23 N-myc amplified neuroblastoma (NB), 11 EWS-FLI1 rearranged Ewing's family of tumor (EFT), 7 SYT-SSX1 rearranged synovial sarcoma (SS), 5 embryonal rhabdomyosarcoma (ERMS), 10 Wilms' tumor (WT), and 5 B-acute lymphoblastic leukemia (B-ALL). Immunostaining was performed per the institutional protocol. GATA3 and ISL1 nuclear staining were scored semiqualitatively for its intensity (weak=1; moderate=2; strong=3) and proportion of positivity (1% to 10%=1; 11% to 25%=2; 26% to 50%=3; >50%=4).

Results: The results of the immunohistochemistry are illustrated in Table 1.

Tumor Type	GATA3 Positive	ISL1 Positive
Neuroblastoma (n=23)	23 (100%)	22 (96%)
Wilms' Tumor (n=10)	0 (0%)	0 (0%)
Embryonal Rhabdomyosarcoma (n=5)	0 (0%)	3 (60%)
Ewing's Family of Tumor (n=11)	0 (0%)	0 (0%)
Synovial Sarcoma (n=7)	0 (0%)	1 (14%)
B-Acute Lymphoblastic Leukemia (n=5)	1 (20%)	0 (0%)

Conclusions: 1. Inclusion of GATA3 and ISL1 to the SBRCT panel adds significant diagnostic value and may reliably be used as markers of neuroblastic lineage.

2. Furthermore, dual positivity helps in challenging scenarios, when there is unequivocal imaging and overlapping IHC findings, limited specimen, and facilty for molecular work up is not available.

1862 Neuroblastic Tumors with Expression of Disialoglycosphingolipids GD2 and/or GD3

Haruna Nishimaki[1], Yoko Nakanishi[2], Shinobu Masuda[3]
[1]Nihon University School of Medicine, Itabashi-ku, Tokyo, Japan, [2]Nihon University School of Medicine, Oyaguchi Kami-cho, Tokyo, Japan, [3]Itabashi-Ku, Tokyo, Japan

Disclosures: Haruna Nishimaki: None; Shinobu Masuda: None

Background: Neuroblastic tumors (NT), including neuroblastoma (GN), ganglioblastoma (GNB), and neuroblastoma (NB), is a solid tumor common in childhood. Recently monoclonal antibodies against disialoglycosphingolipids (GD2), ch14.18, was developed, and it is expected to benefit NB patients. We aimed to clarify the characteristics of clinicopathological features of NTs with GD2 and its precursor GD3 expression, and to clarify the relation with glicosyltransferase in NTs.

Design: Thirty four NTs was investigated for GD2 and GD3 expression analyzed by immunohistochemistry (IHC), and mRNA expression levels of glycosyltransferases (ST3GAL5, ST8SIA1, B4GALNT1 and B3GALT4) measured by qRT-PCR using TaqMan © probes. GD2 and GD3 were expressed in the cytoplasm and nucleus. Multivariate analysis was performed on the intracellular localization and clinicopathological factors of GD2 and GD3. IHC was performed by single staining for GD2 or GD3, and by double staining for GD2 and GD3 analyzed by VECTRA and InForm software.

Results: There was a significant difference between GD2 nuclear expression and the COG high risk group. GD2 nuclear positive cases tended to be GD3 cytoplasm negative (Group 1). On the other hand, GD2 nuclear negative cases tended to be positive for GD3 cytoplasm (Group 3). The relationship between intracellular colocalization and clinical factors was examined using multiple fluorescent staining. As a result, cases with fewer cells single expression of GD3 in the cytoplasm tend to be in INSS stage 4, UH group and COG high risk group. B3GALT4 mRNA expression level was higher in Group 3 (P = 0.021). The mRNA expression levels of B4GALNT1 and B3GALT4 were

higher in Group 1 (P = 0.024, P = 0.013). pNTs with GD2 nuclear localization had high mRNA expression levels of B4GALNT1 and B3GALT4.

Figure 1 - 1862

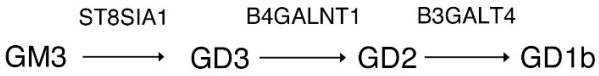

Figure 2 - 1862

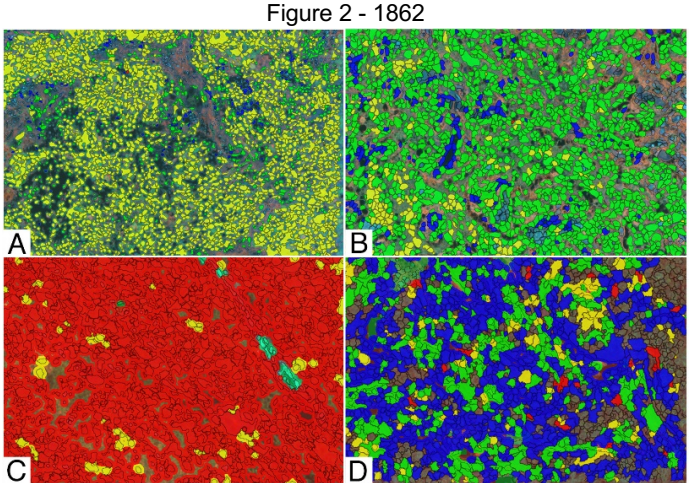

Conclusions: We assume from these results that a translocation of GD3 from cytoplasm to the nucleus as GD2 is predictive of worse outcome, and that lower expression of GD3 in the cytoplasm lacking GD2 is a predictive of a poor prognosis. In conclusion, NTs with GD3 expression had distinct clinicopathological characteristics from NTs with GD2 expression.

1863 Chronic Histiocytic Intervillositis: Clinical and Pathologic Characteristics in a Series of Cases

Andrew Norgan[1], Elizabeth Cheek[1], Reade Quinton[1]
[1]Mayo Clinic, Rochester, MN

Disclosures: Andrew Norgan: None; Elizabeth Cheek: None; Reade Quinton: None

Background: Chronic histiocytic intervillositis (CHIV) is a rare placental lesion of unknown etiology. CHIV is associated with poor pregnancy outcomes, including preterm delivery, spontaneous abortion, intrauterine growth restriction (IUGR) and recurrence in future pregnancies. Although etiologically undefined, prior studies have proposed an autoimmune origin.

Design: In order to further describe the clinical and pathologic characteristics of this rare disease, we performed a retrospective case review of archived placental pathology cases and associated medical records at our institution.

Results: Of 10,087 placentas received in anatomic pathology during the study period, 21 had a diagnosis of isolated CHIV or CHIV in conjunction with other placental pathology (Figure 1). Of the 21 cases, 8 (38%) were from primigravid women and 13 from multigravid women (62%). Women older than 29 years constituted 85% of the cases (18 of 21; mean 32.2 +/- 4.7 years), and 33% were classified as advanced maternal age (>34 years; 7 of 21). By comparison, in an adjacent county in the period from 2012 to 2016, only 52.1% of births were to women with an age >29 years and 15.6% were to women with age >34 years. A concomitant maternal autoimmune disorder (e.g., hypothyroidism, type 1 diabetes) was present in 7 of 21 cases (33%) and preeclampsia was diagnosed in 12 of 21 cases (57%). Pregnancy outcomes included intrauterine fetal demise (10%; 2 of 21 cases) and IUGR in 5 of 19 cases (26%). Preterm premature rupture of membranes in 10 of 19 cases (52%), compared with underlying prematurity rates (in the period 2012 – 2016) of 7%, 8.6% and 9.6% in the adjacent county, state, and United States, respectively.

Pathologically, 11 of 21 study placentas were small for gestational age. Placentas showed a spectrum of involvement by CHIV, with 8 of 21 displaying only focal collections of intervillous histocytes, 4 of 21 minimal but diffuse involvement, and 9 of 21 displaying moderate diffuse involvement (Figure 2). There was no apparent significant difference in neonatal outcomes associated with the observed pathologic severity of the lesion (Table 1). Of note, cases with concomitant chronic villitis were not excluded from this analysis, and chronic villitis was present in half of the cases (11 of 21).

Feature	CHIV Involvement						*P*
	Rare (n=8)		Diffuse Low (n=4)		Diffuse Moderate (n=9)		
	Mean	*SD*	*Mean*	*SD*	*Mean*	*SD*	
Maternal Age (years)	34	3.3	27.75	7.72	32.67	3.28	NT
Gravida	2.38	1.19	2.25	1.26	2.5	1.93	NT
Gestational Age (weeks)	32.38	7.74	37.25	0.96	32.11	5.71	NT
APGAR (1m)	8	1.41	7.33	2.89	5.86	2.91	NT
APGAR (5m)	8.71	0.49	8.33	1.15	6.86	2.73	NT
Fetal WT (g)	2342.86	955.47	3050	717.15	1954.29	1117.69	NT
Placental WT (g)	358.88	191.72	396.75	64.56	279.56	107.85	NT
	%		%		%		
Autoimmune Condition	62		25		11		0.075
Chronic Villitis	75		75		22		0.057
IUFD	12		0		12		NT
IUGR	12		25		38		NT
PPROM	29		25		57		NT
Preeclampsia	38		50		78		0.234
Tobacco Use	25		25		25		NT
Ultrasound Abnormality	25		25		12		NT

Figure 1 - 1863

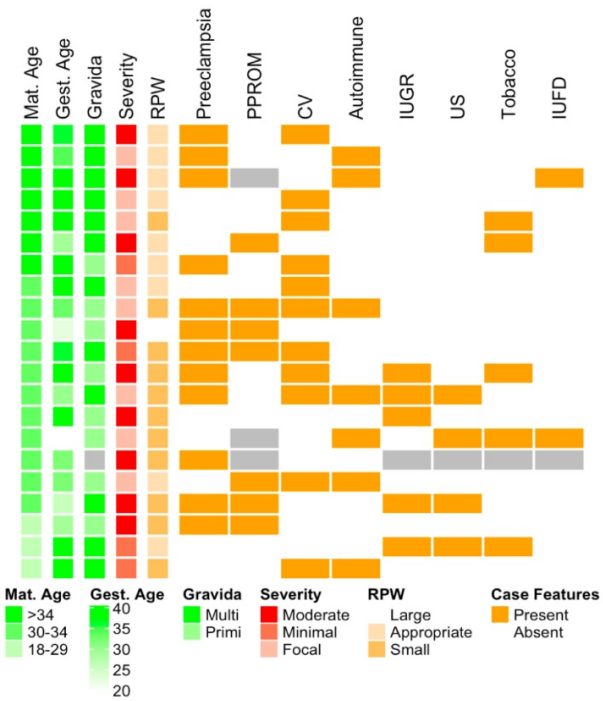

Figure 2 - 1863

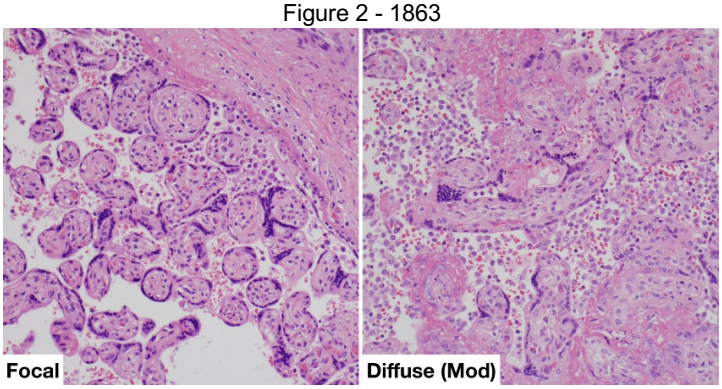

Conclusions: Chronic histiocytic intervillositis remains a cryptic and rarely diagnosed lesion of the placenta, but is an important cause of fetal demise, IUGR, and pre-term birth with a potential for recurrence.

1864 BRAF Point Mutations and Fusions in Mesenchymal Tumors with Clinicopathologic Features Overlapping with Infantile Fibrosarcoma

Alyssa Penning[1], Michael Michal[2], Brandon Larsen[3], Soo-Jin Cho[4], Christina Lockwood[5], Monika Davare[1], Lukas Plank[6], Karen Fritchie[7], Erin Rudzinski[8], Jessica Davis[1]

[1]Oregon Health & Science University, Portland, OR, [2]Biopticka Laborator Ltd., Plzen, Czech Republic, [3]Mayo Clinic, Scottsdale, AZ, [4]University of California San Francisco, San Francisco, CA, [5]University of Washington Medical Center, Seattle, WA, [6]Comenius University Jessenius Medical Faculty, Martin, Slovakia, [7]Mayo Clinic, Rochester, MN, [8]Seattle Children's Hospital, Seattle, WA

Disclosures: Alyssa Penning: None; Michael Michal: None; Brandon Larsen: None; Soo-Jin Cho: *Stock Ownership*, BHB Therapeutics; Christina Lockwood: None; Monika Davare: None; Lukas Plank: None; Karen Fritchie: None; Erin Rudzinski: None; Jessica Davis: *Advisory Board Member*, Bayer Pharmaceuticals/Loxo Oncology

Background: Infantile fibrosarcoma (IFS)/cellular congenital mesoblastic nephroma (cCMN) commonly harbors the classic *ETV6-NTRK3* translocation. However, recent data have demonstrated mesenchymal tumors with IFS-like morphology that harbor fusions in other receptor tyrosine kinases or downstream effectors, including variant *NTRK1/2/3* fusions, and translocations involving *MET*, *RET*, and *BRAF*. Discovery of these additional molecular drivers contributes to a more integrated diagnostic approach and presents potentially important targets for therapy. We report the clinicopathological and molecular features of 10 *BRAF*-altered IFS-like mesenchymal tumors including 6 novel fusions, and for the first time, 4 novel *BRAF* point mutations.

Design: Two index cases (case 1, 2) were identified during a previously published study examining pediatric "ETV6-negative" tumors with IFS morphology. Eight subsequent cases were identified during routine clinical practice. IHC for CD34, S100, and SMA was performed using commercially available antibodies and routine laboratory protocols. Next generation sequencing (NGS) was performed on all cases; the assays varied by institution. All assays included targeted DNA sequencing with either DNA or RNA sequencing for fusion detection.

Results: Of 10 *BRAF*-altered tumors, 4 contained *BRAF* point mutations and 6 harbored one or multiple *BRAF* fusion transcripts (Table 1); all suggestive of resultant constitutive BRAF activation. One harbored 2 *BRAF* fusions (*FOXN3-BRAF, TRIPP1-BRAF*) and another harbored 3 unique transcripts of *EPB41L2-BRAF*. Tumors occurred in 8 males and 2 females, aged from birth to 32 years (median 6 months). Nine were soft tissue based, of which there was a predilection for axial sites; one tumor was in the kidney (cCMN). All neoplasms demonstrated ovoid to short spindle cells arranged in intersecting fascicles or were focally storiform, often with collagenized stroma. Several cases contained branching, ectatic vessels. No specific immunophenotype was observed with variable expression of CD34, S100, and SMA (Table 1).

Case	Age	Sex	Site	Genetics	IHC			Mitosis /10 HPF	LR	Mets	Outcome	Follow-up length
					CD34	S100	SMA					
1	Congenital	M	Paraspinal	BRAFp.L458F	-	+	Patchy +	N/A	N/A	N/A	IUFD at 29 weeks GA	N/A
2	9 days	M	Perirectal	BRAFp.V600D	Focal+	Patchy +	+	10	UNK	UNK	UNK	UNK
3	9 months	F	Neck	BRAFp.V600E	+	-	UNK	1	NO	NO	NED	3 months
4	18 months	F	Kidney, cCMN	BRAFp.V600E	-	Patchy +	-	3	NO	NO	NED	2 years
5	Congenital	M	Scalp	EPB41L2-BRAF^	Focal+	Focal+	Patchy +	1	NO	NO	AWD	5 years
6	3 months	M	Spine, extradural	KIAA1549-BRAF	-	-	-	6	NO	NO	NED	<1 year
7	5 months	M	RP	OSBP-BRAF	-	-	-	1	NO	NO	NED	< 1 year
8	7 months	M	Arm	DAAM1-BRAF	-	-	-	1	NO	NO	NED	< 1 year
9	15 years	M	Leg	TEX41-BRAF	Patchy +	-	++	1	N/A	NO	NED	1 year
10	32 years	M	RP	FOXN3-BRAF, TRIPP1-BRAF	-	-	-	10	N/A*	YES	DOD	9 months

IHC, immunohistochemistry; LR, local recurrence; Mets, metastases; M, male; F, female; cCMN, cellular congenital mesoblastic nephroma; RP, retroperitoneum; N/A, not applicable; IUFD, intrauterine fetal demine; GA, gestational age; AWD, alive with disease; NED, no evidence of disease; DOD, dead of disease; UNK, unknown; ^, contained 3 different EPB41L2-BRAF fusion transcripts, *unresectable at presentation with involvement of kidney and liver

Conclusions: We present the largest cohort of *BRAF*-altered spindle cell neoplasms with IFS-like morphology to date, including novel presentation of point mutations in *BRAF* as oncogenic drivers for these tumors and 6 novel BRAF fusion partners. The identification of point mutations in these tumors highlights a potential gap in current routine diagnostic testing when RNA-sequencing based fusion detection assays alone are employed.

1865 Maternal Hematologic Neoplasms during Pregnancy: Review of Placental Findings

Ashlie Rubrecht[1], Robert Seifert[2], Archana Shenoy[1]
[1]University of Florida, Gainesville, FL, [2]Department of Pathology, Immunology and Lab Medicine, University of Florida, Gainesville, FL

Disclosures: Ashlie Rubrecht: None; Robert Seifert: None; Archana Shenoy: None

Background: Placental metastasis of maternal malignancies is well documented in solid tumors, notably melanoma, which has a propensity for fetal transmission. However, placental and fetal transmission of hematologic neoplasms is not as well documented. In this study, we reviewed placental findings from deliveries with a documented maternal hematologic neoplasm complicating pregnancy aiming to recognize the prevalence of placental transmission and patterns of insufficiency.

Design: Our electronic database (06/11 – 06/19) was queried for patients who had a hematologic neoplasm during pregnancy/at delivery in whom the placenta was examined in pathology. A chart review was performed for patient diagnosis and other historical data including neonatal follow up. Placental slides (Hematoxylin and Eosin as well as applicable immunohistochemical stains) were examined by two practicing and one trainee pathologist for i) Involvement of Hematologic Neoplasm ii) Placenta Pathology in accordance with Amsterdam Placental Workshop Group Consensus Guidelines.

Results: In the 8-year study period, 7012 placentas were examined in pathology. 12 cases fulfilled study criteria, after excluding 1 case that was received fragmented (from termination), 11 cases were included in the study (Table 1). Acute myeloid leukemia was the most common diagnosis (4/11, 36%). Seven cases (63%) showed no histologic evidence of placental spread of neoplasm. Four cases (36%) showed placental spread of neoplasm, however, it was restricted to the maternal compartment. Eight of eleven (72%) cases showed evidence of maternal vascular malperfusion, of which one case also demonstrated fetal vascular malperfusion. Neonatal follow up was available in 10 cases (Age range: 2 days – 5 years), all children alive and well, with blood counts available on 8 cases.

Table 1. Summary of Placental Findings. MVM = Maternal Vascular Malperfusion. FVM = Fetal Vascular Malperfusion. CBC = Complete Blood Count; CBC Units: WBC – thousand/mm^3, Hgb – g/dL, platelets – thousand/mm^3

Case	Diagnosis	Time of Diagnosis	Gestational Age at Delivery	Placental Involvement	Weight, other placental findings	CBC at birth	Follow up, duration
1	Anaplastic large cell lymphoma	20 weeks gestation	33 weeks	None	<10th percentile MVM	WBC: 11.6 Hgb:14.9 Platelets:427	Alive and well, 22 months
2	Acute myeloid leukemia t(8;21)	17 weeks gestation	28 weeks	None	50-75th percentile MVM Focal low grade chronic villitis	WBC: 13.7 Hgb:12.1 Platelets:309	Alive and well, 3 years
3	Chronic myeloid leukemia	Prior to pregnancy	35 weeks	Intervillous space	50-75th percentile MVM	WBC:10.5 Hgb:18.0 Platelets:360	Alive and well, 3 weeks
4	Chronic myeloid leukemia	Prior to pregnancy	32 weeks	Intervillous space	>97th percentile	WBC:5.8 (L) Hgb:10.6 Platelets:246	Alive and well, 5 weeks
5	Myelodysplastic syndrome/Acute myeloid leukemia (monosomy 7)	Prior to pregnancy	30 weeks	Intervillous space Maternal basal plate	50-75th percentile MVM Chronic deciduitis	WBC:9.2 Hgb:10.2(L) Platelets:227	Alive and well, 5 years
6	Hodgkin Lymphoma	Prior to pregnancy	39 weeks 6 days	None	50-75th percentile Chorioamnionitis (Maternal Stage 1, Grade 1) MVM FVM	Not performed	Alive and well, 4 years
7	Mastocytosis	Prior to pregnancy	37 weeks 3 days	None	10-25th percentile Focal low grade chronic villitis Intervillous thrombus	WBC: 16.5 Hgb:16.7 Platelets:254	Alive and well, 14 months
8	Acute myeloid leukemia t(8;16)	31 weeks gestation	31 weeks 5 days	None	50-75th percentile MVM	WBC:7.0 Hgb:12.7 37 Platelets:196	Alive and well, 5.5 weeks
9	Acute promyelocytic leukemia	36 weeks gestation	37 weeks 2 days	Intervillous space Maternal basal plate	<10th percentile MVM	Not performed	Alive and well, 2 days
10	Acute lymphoblastic leukemia, B-cell	28 weeks gestation	34 weeks 2 days	None	75-90th percentile MVM Intervillous thrombus	WBC:9.1 Hgb:14.6 Platelets:243	Alive and well, 2 weeks
11	Anaplastic large cell lymphoma	Immediately postpartum	32 weeks	None	None	Not available	Not available

Conclusions: The study demonstrates that maternal hematologic neoplasms can involve the placenta, however, involvement is typically restricted to the maternal compartment. Maternal vascular malperfusion was a common pattern of placental insufficiency documented. Neonatal outcomes (short-term) were generally favorable.

1866 Civatte Bodies in Pediatric Esophageal Biopsies: Does Lichen Esophagitis Pattern Occur in Children?

Mario Saab-Chalhoub[1], Hernan Correa[1], Julia Anderson[1], Alexandra Kovach[1], Safia Salaria[1]
[1]Vanderbilt University Medical Center, Nashville, TN

Disclosures: Mario Saab-Chalhoub: None; Hernan Correa: None; Alexandra Kovach: None; Safia Salaria: None

Background: Civatte bodies (CBs), apoptotic squamous cells, are associated with lichen planus (LP) of skin and mucosa and, in adults, with Lichen Esophagitis Pattern (LEP). LEP is not well described in children. We characterized clinicopathologic associations of esophageal CBs (ECBs) in children to determine whether LEP occurs in children.

Design: Pathology records (1999-2019) were queried for pediatric patients (pts) whose esophageal biopsy (bx) diagnoses contain keywords “CB,” “apoptosis, “necrosis,” or “dyskeratosis.” Cases with concurrent active eosinophilic (EoE) and acute esophagitis were excluded. H&E slides were reviewed by 3 pathologists and clinical and endoscopic data reviewed.

Results: ECBs meeting inclusion criteria were identified in bxs from 15 pts: 12 male (80%), median age 13 years (range 6-18 years), 8 (53%) prescribed >3 medications, 5 (33%) with Crohn's disease, 4 (27%) suspected or confirmed celiac disease, 4 skin or mucosal findings (3 rash, 1 conjunctival injection), 2 (13%) upper gastrointestinal (GI) dysmotility, and 1 (7%) history of EoE. No pts carried a diagnosis of LP. Clinical indications included variable upper and lower GI symptoms [abdominal pain (9, 75%), vomiting (6, 40%), diarrhea (6, 40%), and constipation (2, 13%)]. Endoscopic findings were mostly normal [12 (80%); white discoloration was noted in 2 (13%) pts and distal erosions in 1 (7%). Histologically, ECBs were present distally in all 15 cases (100%), 4 of which (27%) also had mid ECBs. ECBs were generally focal within the bxs, as isolated 1-3 cells [10 (66%)] or clusters of 4-25 cells, some without inflammation [5 (34%), Figure 1]. Chronic inflammation reminiscent of LEP was present in 7 cases (46%, Figure 2); other cases [8 (53%)] showed no inflammation or spongiosis. Follow-up esophageal bx was reported for 1 pt, which was normal.

Figure 1 - 1866

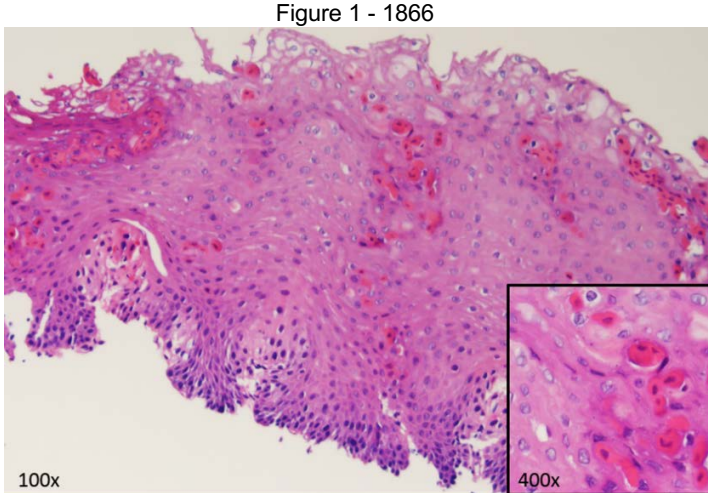

Figure 2 - 1866

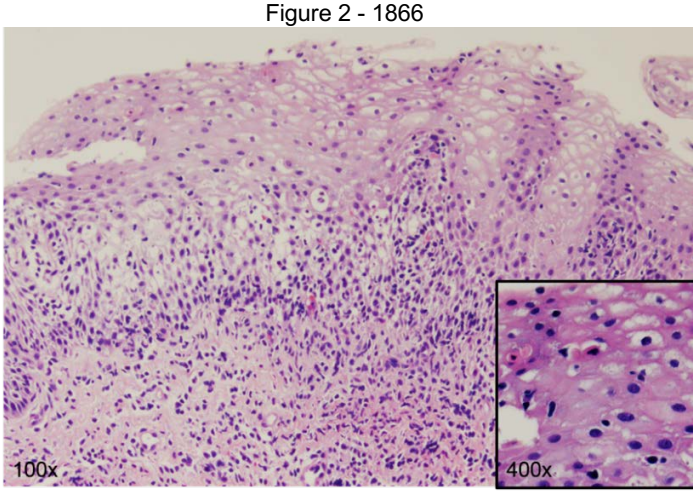

Conclusions: ECBs from pediatric pts may be underrecognized and/or mislabeled as dyskeratosis. Our cohort suggests that pediatric ECBs may be associated with Crohn's disease, polypharmacy, and male sex. In contrast to histologic features in adult-type LEP, which report near-universal chronic inflammation, pediatric ECBs may manifest similarly or as clusters without inflammation such that the epidemiology of pediatric LEP remains unknown. Careful documentation of ECBs in children are needed to improve understanding of their clinical significance.

1867 Villitis of Unknown Etiology, a Placental Reaction to Adverse Fetal Outcome

Qandeel Sadiq[1], Sonali Lanjewar[1], Radhika Sekhri[1], Ava Bhattarai[1]
[1]University of Tennessee Health Science Center, Memphis, TN

Disclosures: Qandeel Sadiq: None; Sonali Lanjewar: None; Radhika Sekhri: None; Ava Bhattarai: None

Background: Villitis of unknown etiology (VUE), is a chorionic villous mononuclear inflammation comprised of lymphocytes and histiocytes. Classically described in term placentas, VUE is noted to occur at the rate of 2 to 33.8 %. Amsterdam placental workshop group grades VUE based on strict morphologic criteria, into low grade and high grade VUE. Of particular importance is high grade VUE, which is associated with adverse fetal outcome. Our goal is to determine the incidence of this lesion in our specific demographic region, determine its clinical associations and fetal outcome.

Design: A total of 17 cases of VUE (15 in singleton placenta and 2 in twin placenta) were identified from search of pathology department database at our institute. Medical charts were reviewed to note clinical associations/ presentation and fetal outcome. VUE was categorized as low grade when inflammation was identified in fewer than 10 contiguous villi in more than one focus, whereas the presence of inflammation affecting multiple foci, on more than one section, with at least one focus affecting more than 10 contiguous villi, was diagnosed as high grade VUE. The C4d was performed to evaluate hypothesis of maternal allograft rejection.

Results: The incidence of VUE in our institute was 2.1%. VUE was encountered in women, < 30 years, at the rate of 88%. Preterm delivery was observed in 41% women. Four major clinical association of VUE include, preeclampsia (41%), morbid obesity (17%), oligohydramnios (17%) and diabetes (11%). High grade VUE was observed in 70.5% of placenta, 64% of which showed chronic histiocytic intervillositis (CHI) and 11% showed maternal floor infarction. Forty one percent of fetuses had intrauterine growth restriction (IUGR), 43% observed in low grade VUE and 57% in high grade. All twin placentas, showed involvement of single placental disc (100%). The C4d showed positivity in 95% of cases.

No. of cases	Age range in years	Preeclampsia	Diabetes	Obesity	Oligo	Preterm delivery	LPW	IUGR	HG-VUE	LG-VUE	B-VUE	CHI	SV-VUE	MFI
17	19-42 (26.4)	7/17	2/17	3/17	3/17	7/17	6/17	7/17	12/17	5/17	9/17	7/17	6/17	2/17

Olgo: Oligohydramnios, LPW: Low placental weight, IUGR: Intrauterine growth restriction, HG-VUE: high grade VUE, LG-VUE: low grade VUE, B-VUE: Basal villi VUE, SV-VUE: Stem villi VUE, MFI: Maternal floor infarction.

Figure 1 - 1867

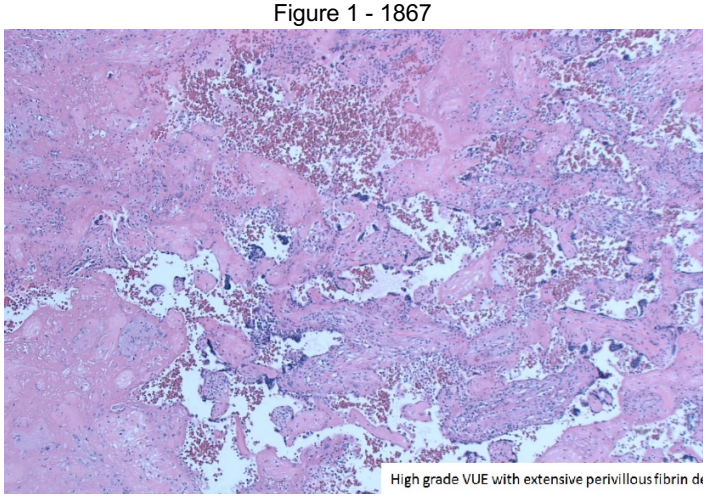

Figure 2 - 1867

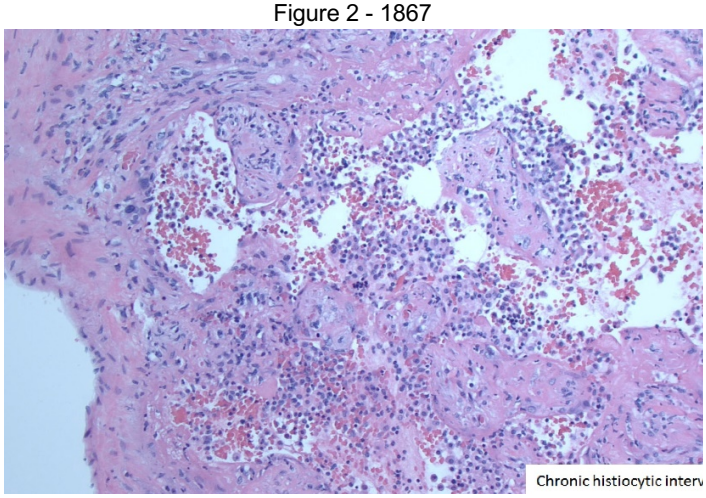

Conclusions: We found a high co-occurrence of CHI and high grade VUE in our IUGR cases, suggesting that these lesions may represent changes seen in the same disease spectrum. Our study also showed particularly high rate of IUGR in low grade VUE. Although possibility of high grade VUE in un-sampled placental tissue could not be excluded, knowledge of association of IUGR with low grade VUE, is essential among the pathologists and clinicians for identification of high risk pregnancies. C4d positivity in majority of placentas supports the theory of maternal allograft rejection in VUE, irrespective of its grade/severity.

1868 Expanding the Differential in Refractory Suspected Germ Cell Tumors

Adeline Yang[1], Tara Pavlock[2], Alison Patterson[2], Theodore Laetsch[3], Dinesh Rakheja[3]
[1]Dallas, TX, [2]Children's Health, Dallas, TX, [3]University of Texas Southwestern Medical Center, Dallas, TX

Disclosures: Adeline Yang: None; Tara Pavlock: None; Alison Patterson: None; Theodore Laetsch: *Consultant*, Bayer; *Grant or Research Support*, Bayer; *Grant or Research Support*, Pfizer; *Consultant*, Novartis; Dinesh Rakheja: None

Background: Germ cell tumors (GCT) account for 7% of all cancer diagnoses among children younger than 20 years, with yolk sac tumors (YST) being the most common. In general, GCTs are highly responsive to cisplatin-based therapy. However, standard regimens fail to cure 10-20% of patients. Patients with treatment refractory or multiply relapsed disease need novel approaches to therapy and may merit re-evaluation of their tumor histology and diagnosis.

Design: Patients were enrolled to a Phase II study of sirolimus+erlotinib for recurrent/refractory germ cell tumors in children, adolescents, and young adults (NCT01962896). Eligibility required histologic verification of an extracranial GCT that was not a pure teratoma/germinoma/seminoma and relapsed/refractory disease following at least 2 prior platinum-containing regimens. Here we review the pathologic features of tumors from patients considered to have refractory GCTs enrolled to this study.

Results: 5 patients were screened for this study between 2014 and 2017. 4 patients were enrolled, while 1 died because of rapid progression of disease prior to enrollment. The median age at diagnosis was 12 years (range: 6-18 years). Original diagnoses were YST in 4 patients and choriocarcinoma in 1 patient. 3 patients had metastases at the time of diagnosis. The median number of pre-study treatment regimens was 5 (range: 4-7), with all receiving BEP and autologous stem cell transplant. Central pathology review on 4 tumors originally diagnosed as YST confirmed the original diagnosis in 2 cases. One case showed nested and acinar morphology with immunoreactivity for trypsin and the diagnosis was revised to AFP-producing pancreatic acinar cell carcinoma (Figure 1). Subsequent NGS showed BRAF PP1CC-BRAF fusion and MYC amplification confirming the revised diagnosis. The 4th tumor showed tubulopapillary morphology and columnar cells with clear cytoplasm. This patient had normal testes, stomach mass and abdominal metastases, and AFP-producing gastric adenocarcinoma was deemed the more appropriate diagnosis (Figure 2).

Figure 1 - 1868

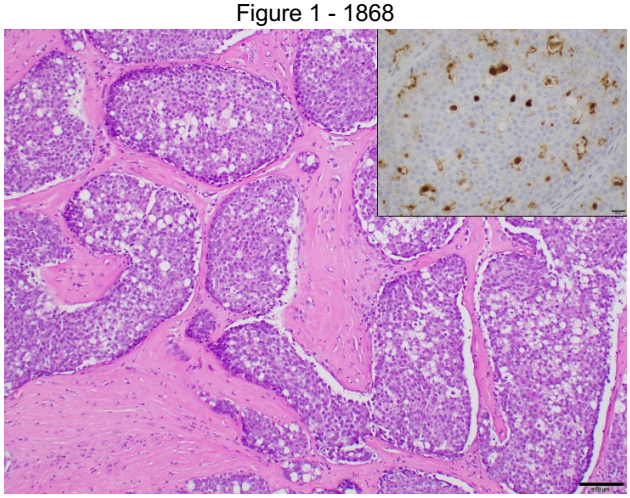

Figure 2 - 1868

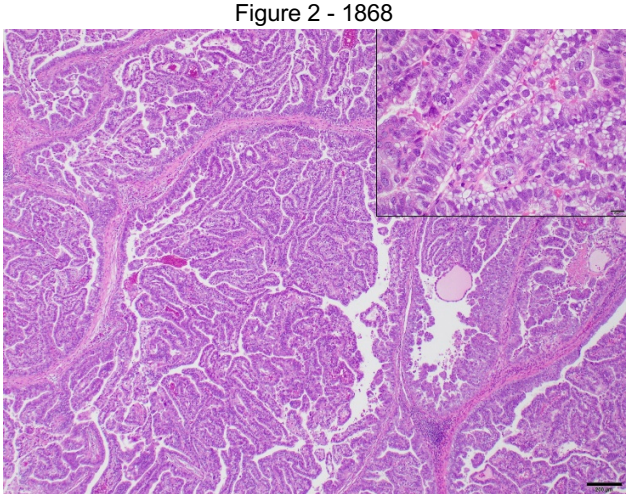

Conclusions: While GCTs are the common AFP and β-hCG secreting neoplasms, suspected GCTs that are recurrent or refractory to standard treatment regimens should raise suspicion for other AFP secreting tumors such as pancreatic and gastric carcinomas and merit histologic re-evaluation.